

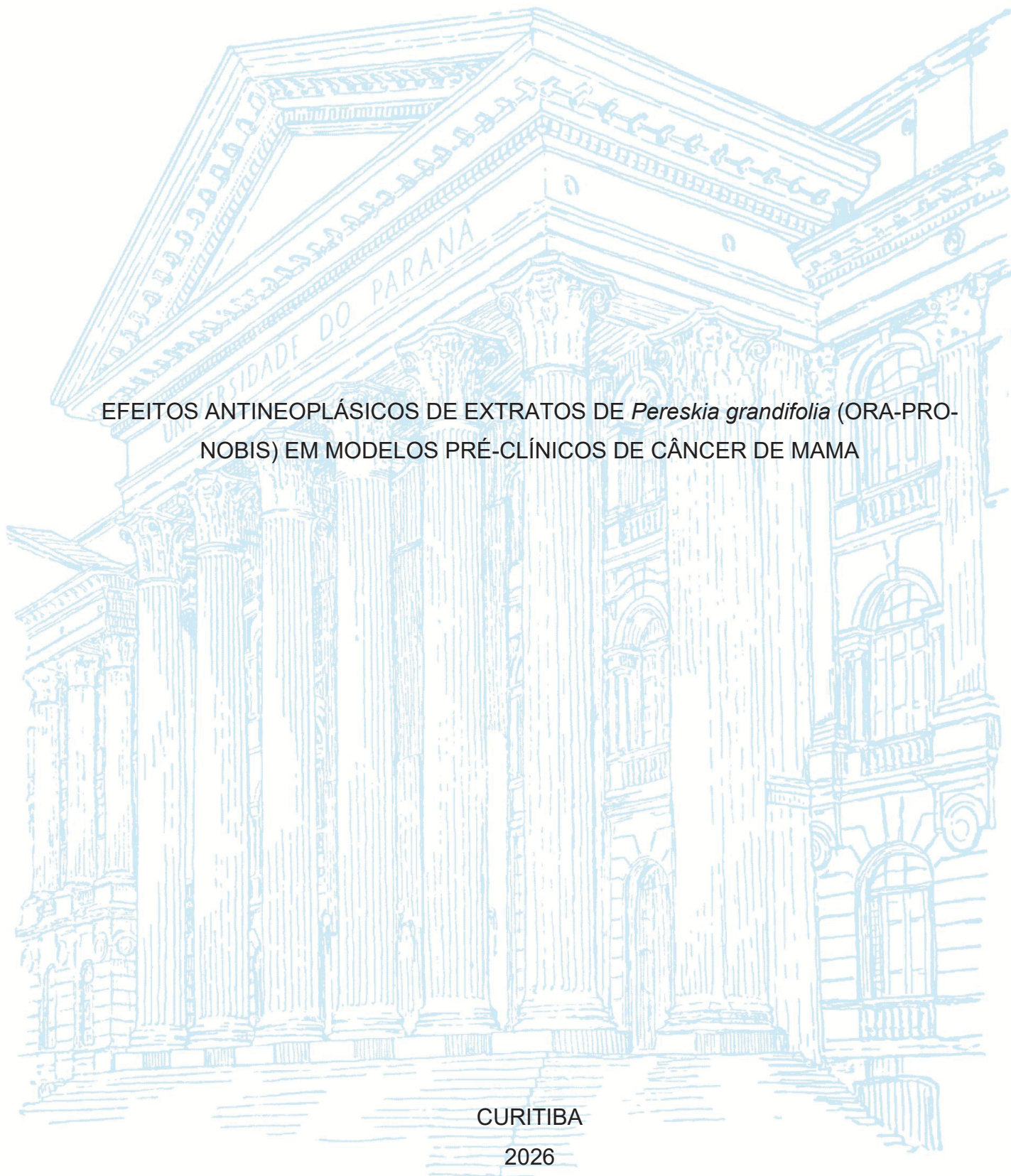
UNIVERSIDADE FEDERAL DO PARANÁ

GABRIELLE OLIVEIRA GUILHERME

EFEITOS ANTINEOPLÁSICOS DE EXTRATOS DE *Pereskia grandifolia* (ORA-PRO-
NOBIS) EM MODELOS PRÉ-CLÍNICOS DE CÂNCER DE MAMA

CURITIBA

2026



GABRIELLE OLIVEIRA GUILHERME

EFEITOS ANTINEOPLÁSICOS DE EXTRATOS DE *Pereskia grandifolia* (ORA-PRO-
NOBIS) EM MODELOS PRÉ-CLÍNICOS DE CÂNCER DE MAMA

Dissertação apresentada ao curso de Pós-Graduação em Farmacologia, Setor de Ciências Biológicas, Universidade Federal do Paraná, como requisito parcial à obtenção do título de Mestre em Farmacologia.

Orientadora: Prof.^a Dr.^a Alexandra Acco

Coorientadora: Dr.^a Maria Carolina Stipp

CURITIBA

2026

DADOS INTERNACIONAIS DE CATALOGAÇÃO NA PUBLICAÇÃO (CIP)
UNIVERSIDADE FEDERAL DO PARANÁ
SISTEMA DE BIBLIOTECAS – BIBLIOTECA DE CIÊNCIAS BIOLÓGICAS

Guilherme, Gabrielle Oliveira, 1998-

Efeitos antineoplásicos de extratos de *Pereskia grandifolia* (ora-pro-nobis) em modelos pré-clínicos de câncer de mama / Gabrielle Oliveira Guilherme. – Curitiba, 2026.
1 recurso on-line : PDF.

Dissertação (Mestrado) – Universidade Federal do Paraná, Setor de Ciências Biológicas, Programa de Pós-Graduação em Farmacologia.

Orientadora: Prof.^a Dr.^a Alexandra Acco.

Coorientadora: Dr.^a Maria Carolina Stipp.

1. Plantas medicinais. 2. Mamas - Câncer. 3. Carcinoma de Ehrlich. 4. Necroptose. 5. Microambiente tumoral. I. Acco, Alexandra., 1972-. II. Stipp, Maria Carolina, 1993-. III. Universidade Federal do Paraná. Setor de Ciências Biológicas. Programa de Pós-Graduação em Farmacologia. IV. Título.

Bibliotecária: Giana Mara Seniski Silva CRB-9/1406



MINISTÉRIO DA EDUCAÇÃO
SETOR DE CIÊNCIAS BIOLÓGICAS
UNIVERSIDADE FEDERAL DO PARANÁ
PRÓ-REITORIA DE PÓS-GRADUAÇÃO
PROGRAMA DE PÓS-GRADUAÇÃO FARMACOLOGIA -
40001016038P0

TERMO DE APROVAÇÃO

Os membros da Banca Examinadora designada pelo Colegiado do Programa de Pós-Graduação FARMACOLOGIA da Universidade Federal do Paraná foram convocados para realizar a arguição da dissertação de Mestrado de **GABRIELLE OLIVEIRA GUILHERME**, intitulada: **Efeitos antineoplásicos de extratos de *Pereskia grandifolia* (ora-pro-nóbis) em modelos pré-clínicos de câncer de mama**, sob orientação da Profa. Dra. ALEXANDRA ACCO, que após terem inquirido a aluna e realizada a avaliação do trabalho, são de parecer pela sua APROVAÇÃO no rito de defesa.

A outorga do título de mestra está sujeita à homologação pelo colegiado, ao atendimento de todas as indicações e correções solicitadas pela banca e ao pleno atendimento das demandas regimentais do Programa de Pós-Graduação.

CURITIBA, 14 de Janeiro de 2026.

Assinatura Eletrônica

16/01/2026 17:41:54.0

ALEXANDRA ACCO

Presidente da Banca Examinadora

Assinatura Eletrônica

19/01/2026 17:22:46.0

LUCIMARA MACH CORTES CORDEIRO

Avaliador Externo (UNIVERSIDADE FEDERAL DO PARANÁ)

Assinatura Eletrônica

19/01/2026 17:22:28.0

STELLE MARCELA PETRIS BISCAIA

Avaliador Externo (UNIVERSIDADE FEDERAL DO PARANÁ)

NOTA EXPLICATIVA

Esta dissertação foi elaborada em formato alternativo, conforme as normas do Programa de Pós-Graduação em Farmacologia da Universidade Federal do Paraná (UFPR). O trabalho é composto por introdução e objetivos, seguidos do artigo científico resultante das atividades desenvolvidas no mestrado, redigido em inglês e formatado de acordo com as diretrizes do periódico ao qual foi submetido.

Inclui, ainda, material suplementar relacionado ao artigo. Ao final, são apresentadas as considerações finais, bem como as referências bibliográficas correspondentes ao manuscrito científico.

AGRADECIMENTOS

Aos meus pais, Márcia e Robson, por todo o esforço e dedicação ao longo da minha formação, sempre priorizando minha educação e me incentivando a seguir meus objetivos. Ao meu irmão, Wellington, que sempre comemorou minhas conquistas e esteve presente em cada passo. Aos meus cachorros, Zeca e Juca, por permanecerem sempre ao meu lado, sendo meu refúgio nos momentos mais difíceis.

Ao meu namorado, Matheus, minha constante em meio ao caos. Obrigada por ser meu porto seguro e morada. Aos meus amigos da Biomedicina (e da vida), obrigada por estarem sempre comigo e tornarem essa jornada muito mais leve.

À minha orientadora prof. Dra. Alexandra Acco, por ter confiado em mim e acreditado no meu potencial. Seu suporte e paciência foram essenciais nesse trabalho. À minha coorientadora, Dra. Maria Carolina Stipp, que, mesmo com a correria, sempre tirava um tempo para me auxiliar nos momentos em que eu me sentia perdida.

Aos meus colegas de laboratório, Bruna, Luana, Kauê, André e Júlia. Sinceramente, faltam palavras para descrever o quanto a amizade de vocês me ajudou a enfrentar a pós-graduação. Vou sentir muita falta dos nossos choros, risadas e fofocas. Espero, de verdade, levar a amizade de vocês para a vida toda.

Aos professores do Departamento de Farmacologia, obrigada por compartilharem seus conhecimentos e por me ensinarem a pensar, de fato, como cientista.

Aos demais colegas do Programa de Pós-Graduação em Farmacologia, pelo convívio diário e aprendizado.

A todos que, direta ou indiretamente, fizeram parte desta caminhada e me ajudaram a evoluir como pessoa e profissional.

À Universidade Federal do Paraná (UFPR), que durante sete anos foi minha segunda casa e base da minha formação.

À CAPES, pelo apoio financeiro concedido para a realização deste trabalho.

“We are the variables. People. We think, we reason, we make choices, we have free will. We can change our destiny.”

Daniel Faraday – Lost

RESUMO

O câncer de mama é a neoplasia maligna mais incidente entre mulheres em todo o mundo, representando um desafio terapêutico relevante, especialmente nos subtipos hormônio-receptor positivos, nos quais a resistência tumoral e a toxicidade dos quimioterápicos convencionais limitam a eficácia clínica. Nesse contexto, a busca por terapias alternativas mais seguras tem impulsionado o interesse por produtos naturais. *Pereskia grandifolia* Haw. (Cactaceae), conhecida como ora-pro-nóbis, apresenta elevado valor nutricional e propriedades biológicas já descritas. Este estudo avaliou a atividade antitumoral e os mecanismos moleculares das frações hidroetanólica (HD) e hexânica (HX) obtidas das folhas de *P. grandifolia*, integrando análises *in vitro* em células MCF-7 e *in vivo* em modelos murinos de carcinoma de Ehrlich (formas sólida e ascítica). A caracterização fitoquímica revelou que a fração HX é predominantemente composta por triterpenos e esteroides, enquanto a fração HD apresentou um perfil químico mais complexo. Em ensaios *in vitro*, a fração HX exibiu citotoxicidade acentuada em células MCF-7, enquanto a fração HD demonstrou efeito antiproliferativo mais pronunciado, sendo ambas capazes de abolir a sobrevivência clonogênica. Para a validação *in vivo*, camundongos fêmeas Swiss inoculados com células de Ehrlich foram tratados por via oral durante 21 dias com HD (100 mg·kg⁻¹), HX (50 mg·kg⁻¹) ou veículo. Ambas as frações inibiram significativamente a progressão do carcinoma sólido de Ehrlich (86% para HD e 89% para HX), sem efeito no modelo ascítico, indicando uma resposta dependente do microambiente tumoral. As análises moleculares por RT-qPCR demonstraram que ambas as frações induziram morte celular programada por necroptose, evidenciada pela modulação de *Ripk1*, *Ripk3* e *Casp8*, além da inibição da angiogênese, indicada pela redução da expressão de *Vegf*. Contudo, os mecanismos antitumorais diferiram entre as frações. A fração HD promoveu uma resposta mais modulada, associada à redução da necrose tumoral, menor infiltração inflamatória e diminuição sistêmica de granulócitos e monócitos circulantes. Em contraste, a fração HX atuou predominantemente como agente citotóxico, induzindo estresse oxidativo, caracterizado pelo aumento de espécies reativas de oxigênio e glutatona reduzida, elevado grau de necrose tumoral, supressão de genes relacionados à inflamação (*Nfkb1*), hipóxia (*Hif1α*) e ciclo celular (*Ccnd1*), além de linfocitose sistêmica. Em conjunto, os resultados demonstram que as frações hidroetanólica e hexânica de *P. grandifolia* apresentam atividade antitumoral relevante em modelos pré-clínicos de câncer de mama sólido, mediada por mecanismos moleculares distintos e complementares. A convergência na indução de necroptose, na inibição da angiogênese e a ausência de toxicidade sistêmica reforçam o potencial da espécie como fonte de compostos bioativos para o desenvolvimento de estratégias terapêuticas antineoplásicas adjuvantes ou alternativas.

Palavras-chave: Plantas medicinais; Neoplasias da Mama; Carcinoma de Ehrlich; Necroptose; Microambiente Tumoral.

ABSTRACT

Breast cancer is the most prevalent malignant neoplasm among women worldwide, representing a significant therapeutic challenge, particularly in hormone receptor–positive subtypes, in which tumor resistance and the toxicity associated with conventional chemotherapeutic agents limit clinical efficacy. In this context, the search for safer alternative therapies has driven growing interest in natural products. *Pereskia grandifolia* Haw. (Cactaceae), commonly known as ora-pro-nóbis, exhibits high nutritional value and well-documented biological properties. This study evaluated the antitumor activity and molecular mechanisms of hydroethanolic (HD) and hexane (HX) fractions obtained from *P. grandifolia* leaves, integrating in vitro analyses using MCF-7 cells and in vivo assays in murine models of Ehrlich carcinoma (solid and ascitic forms). Phytochemical characterization revealed that the HX fraction is predominantly composed of triterpenes and steroids, whereas the HD fraction exhibited a more complex chemical profile. In vitro assays demonstrated that the HX fraction exerted pronounced cytotoxicity in MCF-7 cells, while the HD fraction showed a more marked antiproliferative effect; both fractions were able to abolish clonogenic survival. For in vivo validation, female Swiss mice inoculated with Ehrlich tumor cells were orally treated for 21 days with HD (100 mg·kg⁻¹), HX (50 mg·kg⁻¹), or vehicle. Both fractions significantly inhibited the progression of solid Ehrlich carcinoma (86% for HD and 89% for HX), with no effect observed in the ascitic model, indicating a tumor microenvironment–dependent response. Molecular analyses by RT-qPCR demonstrated that both fractions induced programmed cell death via necroptosis, as evidenced by the modulation of *Ripk1*, *Ripk3*, and *Casp8*, in addition to the inhibition of angiogenesis, indicated by reduced *Vegf* expression. However, distinct antitumor mechanisms were observed between the fractions. The HD fraction promoted a more modulated response, associated with reduced tumor necrosis, lower inflammatory infiltration, and a systemic decrease in circulating granulocytes and monocytes. In contrast, the HX fraction acted predominantly as a cytotoxic agent, inducing oxidative stress characterized by increased reactive oxygen species and reduced glutathione levels, extensive tumor necrosis, suppression of genes related to inflammation (*Nfkb1*), hypoxia (*Hif1α*), and cell cycle regulation (*Ccnd1*), as well as systemic lymphocytosis. Collectively, these findings demonstrate that the hydroethanolic and hexane fractions of *P. grandifolia* exhibit relevant antitumor activity in preclinical models of solid breast cancer, mediated by distinct and complementary molecular mechanisms. The convergence in necroptosis induction and angiogenesis inhibition, together with the absence of systemic toxicity, reinforces the potential of this species as a source of bioactive compounds for the development of adjuvant or alternative antineoplastic therapeutic strategies.

Keywords: Medicinal Plants; Breast Neoplasms; Ehrlich Tumor; Necroptosis; Tumor Microenvironment.

LISTA DE FIGURAS

- Figura 1.** As marcas do câncer: capacidades biológicas adquiridas durante o desenvolvimento tumoral.....17
- Figura 2.** Inflorescência e folhas de um arbusto jovem de *P. grandifolia* destacando a coloração rosa-vibrante das flores e o formato das folhas.....20

ARTÍGO CIENTÍFICO

- Figure 1.** ¹³C NMR Spectrum and DEPT ¹³⁵C NMR Spectrum of the Hexane Extract (HX) of *P. grandifolia*.....37
- Figure 2.** Effect of *Pereskia grandifolia* fractions treatment on MCF-7 cells..39
- Figure 3.** Clonogenic assay in MCF7 cells.....40
- Figure 4.** Effects of *P. grandifolia* extracts on ascitic Ehrlich tumor development.....41
- Figure 5.** Experimental design and effects of *P. grandifolia* on the solid Ehrlich tumor development.....42
- Figure 6.** Histopathological analysis of tumor tissue.....43
- Figure 7.** Oxidative stress parameters in tumor tissues.....44
- Figure 8.** Effects of *P. grandifolia* extracts on expression of genes related to cell death, inflammation, proliferation, and angiogenesis in solid Ehrlich carcinoma.....45
- Supplementary Figure S1.** Assessment of inflammatory markers in Ehrlich solid tumor tissue.....63
- Supplementary Figure S2.** Representative photomicrographs of liver sections from mice bearing Ehrlich solid tumor.64

LISTA DE TABELAS

| | |
|--|----|
| Table 1. Phytochemical screening for the presence of alkaloids, flavonoids, coumarins, steroids, and/or triterpenes of <i>P. grandifolia</i> extracts..... | 36 |
| Table 2. Hematological and biochemical parameters of Ehrlich carcinoma-bearing mice treated with vehicle or <i>P. grandifolia</i> fractions and naïve mice. . | 46 |
| Supplementary Table S1. Mobile phases and detection techniques used for thin-layer chromatography of <i>P. grandifolia</i> extracts. | 61 |
| Supplementary Table S2. Primers used to perform RTqPCR in mice Ehrlich tumor samples..... | 62 |
| Supplementary Table S3. Characterization of secondary metabolites of <i>P. grandifolia</i> extracts by thin-layer chromatography (TLC) assay. | 62 |

LISTA DE ABREVIATURAS OU SIGLAS

- AEC – Carcinoma de Ehrlich Ascítico (do inglês *Ascitic Ehrlich Carcinoma*)
- ALT – Alanina aminotransferase
- ARRIVE – Diretrizes para o Relato de Pesquisas em Animais *In vivo* (do inglês *Animal Research: Reporting of In vivo Experiments*)
- AST – Aspartato aminotransferase
- BC – *Breast Cancer*
- BHT – Butil-hidroxitolueno
- CCD – Cromatografia em Camada Delgada
- CEUA – Comissão de Ética no Uso de Animais
- CM – Câncer de Mama
- Ctrl – Controle (ou Controle Negativo)
- DAMPs – Padrões Moleculares Associados ao Dano (do inglês *Damage-associated molecular patterns*)
- DCFH-DA – Diclorofluoresceína-diacetato
- DMF – N,N-dimetilformamida
- EDTA – Ácido etilenodiaminotetracético
- ER – Receptor de Estrógeno
- ER α – Receptor de Estrógeno alfa
- FBS – Soro Fetal Bovino
- Gran – Granulócitos
- GSH – Glutationa Reduzida
- HBG – Hemoglobina
- HCT – Hematócrito
- HD – Fração Hidroetanólica
- HER2 – Receptor 2 do Fator de Crescimento Epidérmico Humano (do inglês *Human Epidermal Growth Factor Receptor 2*)
- HX – Fração Hexânica
- IC₅₀ – Concentração Inibitória 50%
- IL-1 β – Interleucina-1 beta
- IP – Intraperitoneal
- LPO – Peroxidação Lipídica (do inglês *Lipid Peroxidation*)
- Lymph – Linfócitos (do inglês *Lymphocytes*)

MDSCs – Células Supressoras Derivadas da Linhagem Mieloide (do inglês *Myeloid-derived suppressor cells*)

MEC – Matriz Extracelular

Mon – Monócitos (do inglês *Monocytes*)

MPO – Mieloperoxidase

NAG – N-acetil-beta-D-glucosaminidase

OED – Dose Efetiva Otimizada (do inglês *Optimized Effective Dose*)

PFA – Paraformaldeído

PLT – Plaquetas

PPI – Interação Proteína-Proteína (do inglês *Protein-protein interaction*)

ppm – Partes por milhão

PR – Receptor de Progesterona

RBC – Glóbulos Vermelhos / Hemácias (do inglês *Red Blood Cells*)

RMN ou NMR – Ressonância Magnética Nuclear (do inglês *Nuclear Magnetic Resonance*)

ROS – Espécies Reativas de Oxigênio (do inglês *Reactive Oxygen Species*)

RT-qPCR – Reação em Cadeia da Polimerase em Tempo Real com Transcrição Reversa (do inglês *Quantitative Real-Time PCR*)

SEC – Carcinoma de Ehrlich Sólido (do inglês *Solid Ehrlich Carcinoma*)

SERD – Degradadores Seletivos dos Receptores de Estrogênio

SERM – Moduladores Seletivos dos Receptores de Estrogênio

SOD – Superóxido Dismutase

TAMs – Macrófagos Associados ao Tumor (do inglês *Tumor-associated macrophages*)

TLC – Cromatografia em Camada Delgada (do inglês *Thin-Layer Chromatography*)

TME – Microambiente Tumoral (do inglês *Tumor Microenvironment*)

TMS – Tetrametilsilano

TNF- α – Fator de Necrose Tumoral alfa

WBC – Glóbulos Brancos / Leucócitos (do inglês *White Blood Cells*)

LISTA DE SÍMBOLOS

δ – Deslocamento químico (do inglês *Chemical shift*)

SUMÁRIO

| | |
|--|-----------|
| 1 INTRODUÇÃO | 16 |
| 1.1 CÂNCER DE MAMA: DEFINIÇÃO E INCIDÊNCIA | 16 |
| 1.2 MICROAMBIENTE TUMORAL..... | 16 |
| 1.3 TRATAMENTOS ATUAIS E LIMITAÇÕES | 18 |
| 1.4 PRODUTOS NATURAIS E <i>Pereskia grandifolia</i> | 19 |
| 1.5 MODELO TUMORAL DE EHRLICH..... | 20 |
| 1.6 LINHAGEM CELULAR MCF-7 | 21 |
| 2 OBJETIVOS | 21 |
| 2.1 OBJETIVO GERAL | 21 |
| 2.2 OBJETIVOS ESPECÍFICOS | 21 |
| 3 ARTIGO CIENTIFICO | 23 |
| 1 INTRODUCTION | 26 |
| 2 MATERIAL AND METHODS | 27 |
| 2.1 CHEMICALS AND REAGENTS..... | 27 |
| 2.2 PLANT MATERIAL AND EXTRACTION..... | 28 |
| 2.3 PHYTOCHEMICAL CHARACTERIZATION..... | 29 |
| 2.4 NUCLEAR MAGNETIC RESONANCE SPECTROSCOPIC ANALYSIS OF THE HX EXTRACT | 30 |
| 2.5 <i>IN VITRO</i> BREAST CANCER ASSAYS WITH MCF-7 CELLS | 30 |
| 2.5.1 Cell Viability and Proliferation | 30 |
| 2.5.2 Clonogenic Test..... | 30 |
| 2.6 <i>IN VIVO</i> EHRLICH TUMOR MODELS..... | 31 |
| 2.6.1 Ascitic Ehrlich Tumor in Mice..... | 31 |
| 2.6.2 Solid Ehrlich Carcinoma in Mice | 32 |
| 2.7 HISTOLOGY OF TUMOR AND ORGANS..... | 33 |
| 2.8 OXIDATIVE STRESS PARAMETERS IN TUMOR TISSUE | 33 |
| 2.9 INFLAMMATORY PARAMETERS IN TUMOR TISSUE | 33 |
| 2.10 QUANTITATIVE REAL-TIME PCR AND BIOINFORMATICS | 34 |
| 2.11 BIOCHEMICAL AND HEMATOLOGICAL ASSAYS..... | 35 |
| 2.12 DATA ANALYSIS..... | 35 |
| 3 RESULTS | 35 |

| | |
|---|-----------|
| 3.1 PHYTOCHEMICAL SCREENING AND THIN-LAYER CHROMATOGRAPHY (TLC) SHOWED DIFFERENT COMPOUNDS IN HD AND HX | 35 |
| 3.2 STRUCTURAL IDENTIFICATION BY NMR | 36 |
| 3.3 HX DEMONSTRATES POTENT CYTOTOXICITY AND HD A GREATER ANTIPROLIFERATIVE ACTIVITY IN MCF-7 CELLS | 37 |
| 3.4 HX AND HD REDUCE CLONOGENIC SURVIVAL OF MCF-7 CELLS | 40 |
| 3.5 HD AND HX DO NOT AFFECT ASCITIC TUMOR DEVELOPMENT | 40 |
| 3.6 HD AND HX SUPPRESS SOLID EHRlich TUMOR GROWTH..... | 41 |
| 3.7 HD AND HX INDUCED CHANGES IN TUMOR HISTOLOGY..... | 42 |
| 3.8 HX INDUCES OXIDATIVE STRESS, BUT NEITHER EXTRACT ALTERS TUMOR INFLAMMATORY PARAMETERS..... | 43 |
| 3.9 HD AND HX INDUCE <i>RIPK1/RIPK3</i> -MEDIATED NECROPTOSIS AND SUPPRESS SURVIVAL/PROLIFERATION PATHWAYS..... | 44 |
| 3.10 HD AND HX DID NOT INDUCE SYSTEMIC TOXICITY | 45 |
| 4 DISCUSSION | 47 |
| 5 REFERENCES | 53 |
| 6 SUPPLEMENTARY MATERIAL | 61 |
| 4 CONSIDERAÇÕES FINAIS | 65 |
| 5 REFERÊNCIAS..... | 66 |

1 INTRODUÇÃO

1.1 CÂNCER DE MAMA: DEFINIÇÃO E INCIDÊNCIA

O câncer de mama (CM) é uma doença caracterizada pela proliferação descontrolada de células anormais do tecido mamário, resultando na formação de um tumor com capacidade de invasão e disseminação (INCA, 2023). Trata-se do tipo de câncer mais frequente entre as mulheres em todo o mundo e da principal causa de morte por câncer nessa população, configurando um relevante problema de saúde pública (Łukasiewicz et al., 2021; Dvir et al., 2024).

O CM é uma doença altamente heterogênea, apresentando variações biológicas tanto entre pacientes quanto entre subpopulações celulares dentro de um mesmo tumor (Lüönd et al., 2021). Clinicamente, a expressão de marcadores moleculares específicos permite a classificação do CM em diferentes subtipos, incluindo os tumores receptor hormônio-positivos, caracterizados pela expressão de receptores de estrógeno e/ou progesterona (ER+/PR+), aqueles com superexpressão do receptor do fator de crescimento epidérmico humano 2 (HER2+) e os tumores triplo-negativos, definidos pela ausência da expressão desses receptores (Lüönd et al., 2021; Orrantia-Borunda et al., 2022). O CM triplo negativo representa aproximadamente 15–20% de todos os carcinomas mamários e está, em geral, associado a pior prognóstico, com elevadas taxas de invasão e mortalidade (Yin et al., 2020; Li et al., 2022). Em contraste, o subtipo receptor hormonal positivo apresenta maior prevalência na população e está associado a altas taxas de recidiva (Szostakowska et al., 2018; Li et al., 2024). Diante da heterogeneidade do CM, as terapias também mudam entre os subtipos, como citado adiante.

1.2 MICROAMBIENTE TUMORAL

A interação dinâmica entre as células neoplásicas e o estroma hospedeiro estabelece um microambiente tumoral (TME) permissivo, fundamental para a manutenção da viabilidade celular e disseminação da doença. O estabelecimento desse microambiente favorece a aquisição de capacidades biológicas distintivas que orquestram a transformação maligna e a progressão tumoral, conforme esquematizado na Figura 1 (Hanahan, 2022).

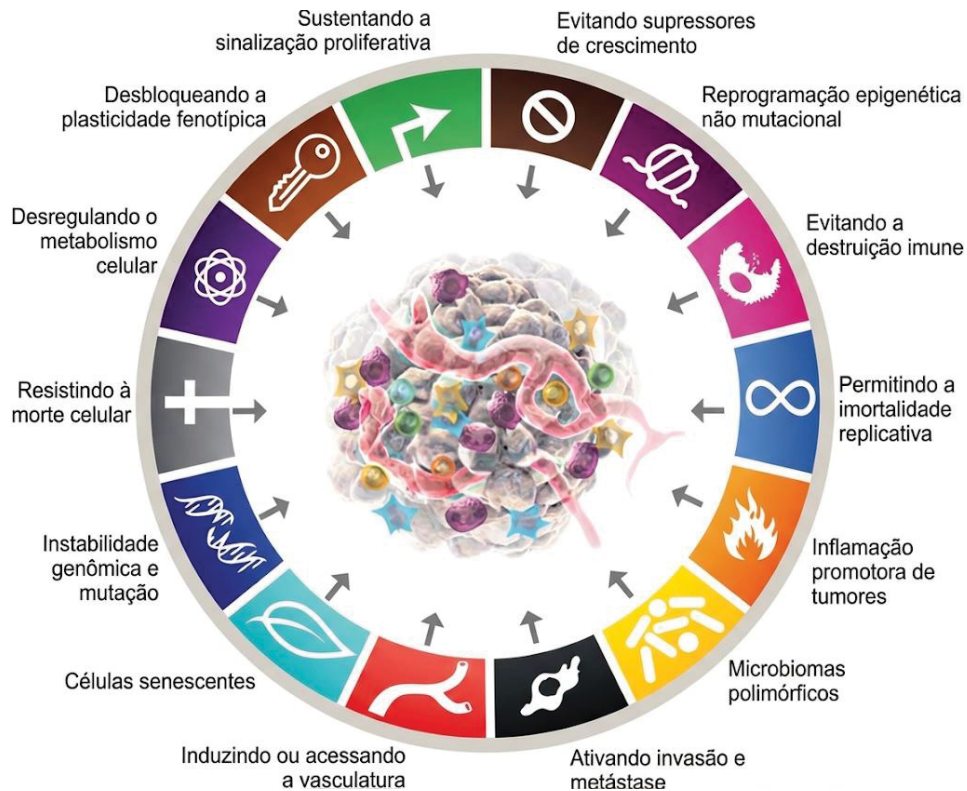


Figura 1. As características fundamentais do câncer: capacidades biológicas adquiridas durante o desenvolvimento tumoral. Fonte: Adaptado de Hanahan (2022).

Como mencionado, o tumor de mama está inserido em um ecossistema complexo e heterogêneo composto por células estromais, proteínas da matriz extracelular (MEC), citocinas, quimiocinas e vesículas extracelulares (Sharma et al., 2025). Nesse contexto, sabe-se que as células cancerosas frequentemente “educam” ou reprogramam as células do hospedeiro para sustentar seu próprio crescimento e disseminação. Células imunes infiltrantes, como os macrófagos associados ao tumor (TAMs) e as células supressoras derivadas da linhagem mieloide (MDSCs), apresentam elevada plasticidade funcional, podendo exercer papéis antitumorais ou pró-tumorais. Contudo, durante a progressão tumoral, observa-se predominantemente um desequilíbrio favorável ao fenótipo pró-tumoral e imunossupressor (Rannikko & Hollmén, 2024; Kundu et al., 2024). Além disso, o microambiente tumoral é caracterizado por um estado de inflamação crônica e desbalanço redox, no qual a secreção persistente de citocinas pró-inflamatórias e o aumento das espécies reativas de oxigênio (ROS) promovem a ativação de vias de sinalização intracelular, como a do NF- κ B (Aboelella et al., 2021; Cao et al., 2024). Conseqüentemente, esse cenário não apenas favorece a progressão da doença,

mas também estabelece mecanismos de proteção celular que dificultam a eficácia das terapias convencionais.

1.3 TRATAMENTOS ATUAIS E LIMITAÇÕES

O tratamento do CM fundamenta-se em uma estratégia multimodal, que combina intervenções locais e sistêmicas. As modalidades terapêuticas incluem a ressecção cirúrgica do tumor primário e a radioterapia, associadas a regimes de quimioterapia, que podem ser administrados em caráter neoadjuvante ou adjuvante - além de terapias endócrinas e terapias alvo-moleculares, prescritas conforme o perfil imuno-histoquímico do tumor (Fisusi & Akala, 2019). No contexto do CM receptor hormonal positivo, as terapias endócrinas constituem o principal pilar do tratamento sistêmico, sendo consideradas o padrão terapêutico nessa condição (Loibl et al., 2021). Essas terapias atuam reduzindo os níveis de estrogênio ou bloqueando a estimulação tumoral mediada por esse hormônio, por meio do uso de inibidores da aromatase (Ex. letrozol e exemestano), moduladores seletivos dos receptores de estrogênio (SERM; Ex. tamoxifeno e toremifeno) ou degradadores seletivos dos receptores de estrogênio (SERD; fulvestranto) (Drăgănescu & Carmocan, 2017). Em casos selecionados, podem ser associadas à quimioterapia, com impacto na redução da mortalidade (Łukasiewicz et al., 2021). O tratamento quimioterápico inclui a aplicação simultânea de 2 a 3 dos seguintes fármacos: carboplatina, ciclofosfamida, 5-fluorouracil/capecitabina, taxanos (paclitaxel, docetaxel) e antraciclinas (doxorubicina, epirrubicina). A escolha do fármaco adequado é de grande importância, uma vez que diferentes subtipos moleculares de câncer de mama respondem de maneira distinta à quimioterapia (Łukasiewicz et al., 2021; Fisher et al., 1998.) Mais recentemente, a terapia biológica com trastuzumabe e pertuzumabe, por exemplo, passou a ser indicada em pacientes com câncer de mama HER2-positivo; enquanto abemaciclibe e everolimo também podem ser utilizados no câncer de mama HER2-negativo e ER-positivo (Kwapisz, 2017; Royce e Osman, 2015; Łukasiewicz et al., 2021).

Entretanto, as terapias atualmente empregadas no tratamento do CM ainda apresentam limitações clínicas relevantes. A eficácia da quimioterapia e das terapias endócrinas pode ser comprometida pelo desenvolvimento de mecanismos de resistência, reduzindo a resposta em longo prazo. Além disso, os eventos adversos associados a esses tratamentos impactam negativamente a qualidade de vida e a

adesão das pacientes (Telang, 2023; Zafar et al., 2025). Esse cenário reforça a necessidade de novas alternativas terapêuticas mais eficazes e menos tóxicas, evidenciando o potencial de compostos bioativos para superar essas limitações.

1.4 PRODUTOS NATURAIS BIOATIVOS E *Pereskia grandifolia*

O estudo de produtos naturais tem se consolidado como uma estratégia promissora na busca por novos fármacos antineoplásicos. Os fitoquímicos representam uma vasta classe de moléculas bioativas capazes de atuar simultaneamente em múltiplos alvos moleculares, favorecendo a modulação de vias de sinalização complexas envolvidas na progressão tumoral e na resistência a fármacos (Devaraji & Thanikachalam, 2025). Fitoquímicos como flavonóides, alcaloides, terpenóides e ácidos fenólicos já demonstraram resultados positivos em ensaios pré-clínicos, com mecanismos envolvendo a inibição da proliferação celular, indução da apoptose, supressão da angiogênese e prevenção de metástases (Zhang et al., 2024).

Nesse contexto, destaca-se a *Pereskia grandifolia* Haw. (Cactaceae). Popularmente vinculada ao grupo das plantas conhecidas como 'ora-pro-nóbis', trata-se de uma espécie nativa da flora brasileira, valorizada pelo alto teor nutricional, e frequentemente utilizada na culinária e na medicina tradicional para o tratamento de diversas enfermidades. Morfologicamente, apresenta folhas ovais constituídas por mucilagem e cristais de oxalato de cálcio, caules dotados de espinhos e inflorescências de coloração rosa ou rosa-escuro (Laverde Junior et al., 2022), conforme ilustração da figura 2. Em estudos prévios, a composição fitoquímica da planta indicou a presença de terpenóides, esteróides, alcaloides e compostos fenólicos, incluindo flavonoides e glicosídeos (Amaral et al., 2025). Adicionalmente, diversas atividades biológicas promissoras já foram descritas em modelos *in vivo* e *in vitro*, tais como propriedades antioxidantes, citotóxicas, antimicrobianas, antiobesidade, diuréticas, hipotensivas, moluscidas, inibidoras da acetilcolinesterase e hepatoprotetoras, somadas a avaliações de sua toxicidade (Albuquerque et al., 2025). Nesse âmbito, Nurestri et al. (2009) conduziram o estudo pioneiro avaliando o potencial citotóxico de diferentes extratos de *P. grandifolia* em linhagens de células cancerosas, incluindo o câncer de mama receptor hormonal positivo. Entretanto, ainda há escassez de dados na literatura, sobretudo em modelos *in vivo*, voltados para a elucidação do potencial e dos mecanismos

antitumorais da espécie, evidenciando a necessidade de investigações complementares. O presente estudo foi executado para preencher, pelo menos em parte, esta lacuna, utilizando modelos *in vitro* e *in vivo* de CM.



Figura 2. Inflorescência e folhas de um arbusto jovem de *P. grandifolia* destacando a coloração rosa-vibrante das flores e o formato das folhas. Fonte: Taylor et al. (2015).

1.5 MODELO TUMORAL DE EHRLICH

O Tumor de Ehrlich é um modelo experimental de neoplasia mamária murina amplamente utilizado em estudos pré-clínicos, permitindo a avaliação da eficácia de agentes antitumorais, bem como de aspectos imunológicos, inflamatórios e comportamentais associados à progressão tumoral (Feitosa et al., 2021). Descrito inicialmente por Paul Ehrlich em 1906 como um adenocarcinoma mamário espontâneo em camundongos, caracteriza-se por elevada capacidade proliferativa, o que possibilitou o estabelecimento de linhagens transplantáveis. Dependendo da via de inoculação, o tumor pode se apresentar na forma ascítica, após inoculação intraperitoneal, ou sólida, quando inoculado por via subcutânea ou intramuscular (Ozaslan et al., 2011; Radulski et al., 2023). Entre suas principais características destacam-se o crescimento rápido, a ausência de regressão espontânea e a alta transplantabilidade em diferentes linhagens de camundongos (Radulski et al., 2023). Em virtude dessas características, particularmente o rápido desenvolvimento e a

reprodutibilidade do modelo, o Carcinoma de Ehrlich foi selecionado para o presente estudo.

1.6 LINHAGEM CELULAR MCF-7

A linhagem MCF-7 consolidou-se como um dos modelos celulares humanos de câncer de mama mais amplamente estudados. Caracterizada pela dependência de estrogênio, tem sido utilizada há mais de quatro décadas como uma ferramenta fundamental para a investigação da biologia tumoral e para a avaliação de novas abordagens terapêuticas (Garroni et al., 2024). Embora tenha sido isolada a partir de um sítio metastático, a MCF-7 apresenta baixo potencial invasivo e agressivo, sendo considerada o modelo clássico para o estudo do câncer de mama receptor hormonal positivo (Comşa et al., 2015).

Em virtude dessas características, que se assemelham às das células de Ehrlich, esta linhagem foi selecionada para investigar os efeitos do tratamento com *P. grandifolia in vitro*.

2 OBJETIVOS

2.1 OBJETIVO GERAL

Avaliar a atividade antitumoral das frações hidroetanólica (HD) e hexânica (HX) das folhas de *P. grandifolia* Haw. em modelo *in vitro*, utilizando a linhagem celular de adenocarcinoma mamário humano (MCF-7), e *in vivo*, no modelo murino de Carcinoma de Ehrlich (nas formas sólida e ascítica), bem como investigar os possíveis mecanismos envolvidos na resposta antineoplásica.

2.2 OBJETIVOS ESPECÍFICOS

1. Obter e caracterizar a fração hidroetanólica (HD) e hexânica (HX) das folhas de *Pereskia grandifolia*, por meio de triagem fitoquímica;
2. Avaliar a citotoxicidade e o potencial antiproliferativo das frações HD e HX na linhagem de adenocarcinoma mamário humano (MCF-7), determinando a viabilidade celular, proliferação e capacidade clonogênica *in vitro*;
3. Investigar a atividade antitumoral *in vivo* no modelo de Carcinoma de Ehrlich na forma ascítica e na forma sólida, monitorando a evolução tumoral;
4. Analisar as características histopatológicas do tecido tumoral;

5. Determinar o efeito dos tratamentos sobre o microambiente tumoral, quantificando biomarcadores de estresse oxidativo e mediadores inflamatórios;
6. Elucidar os possíveis mecanismos de ação molecular por meio da análise da expressão gênica (RT-qPCR) de alvos relacionados à apoptose, autofagia, necroptose, angiogênese e ciclo celular, complementada por análise de bioinformática (redes proteicas - PPI);
7. Verificar a toxicidade sistêmica dos tratamentos nos animais portadores de tumor, por meio da avaliação de parâmetros hematológicos, bioquímicos e histológicos.

3 ARTIGO CIENTIFICO

***Pereskia grandifolia* (ORA-PRO-NOBIS) EXTRACTS EXHIBIT MULTI-TARGED ANTINEOPLASTIC ACTIVITY IN PRECLINICAL MODELS OF BREAST CANCER**

Gabrielle Oliveira Guilherme¹, Suelen C.S. Baal², Bruna Isadora Pilger¹, Julia Helena Carvalho¹, André Felipe Naidek¹, Luana Eloisa Leal¹, Kauê Marcel Oliveira¹, Gabriela Casani Cardoso³, Gustavo Ratti da Silva⁴, Francislaine Aparecida dos Reis Lívero^{1,4}, Cintia Aparecida dos Anjos⁵, Obdulio Gomes Miguel⁵, Edneia Amancio de Souza Ramos³, Jaqueline Carvalho de Oliveira², Maria Carolina Stipp¹, Alexandra Acco^{1*}

¹ Department of Pharmacology, Federal University of Paraná, Curitiba, PR, Brazil.

² Department of Genetics, Federal University of Paraná, Curitiba, PR, Brazil.

³ Department of Basic Pathology, Federal University of Paraná, Curitiba, PR, Brazil.

⁴ Laboratory of Preclinical Research of Natural Products, Paranaense University, Umuarama, PR, Brazil.

⁵ Department of Pharmaceutical Sciences, Federal University of Paraná, Curitiba, PR, Brazil.

* Corresponding author

Department of Pharmacology, Biological Sciences Sector, Federal University of Paraná

PO Box 19031, Curitiba, PR, 81531-980, Brazil.

e-mail: aleacco@ufpr.br

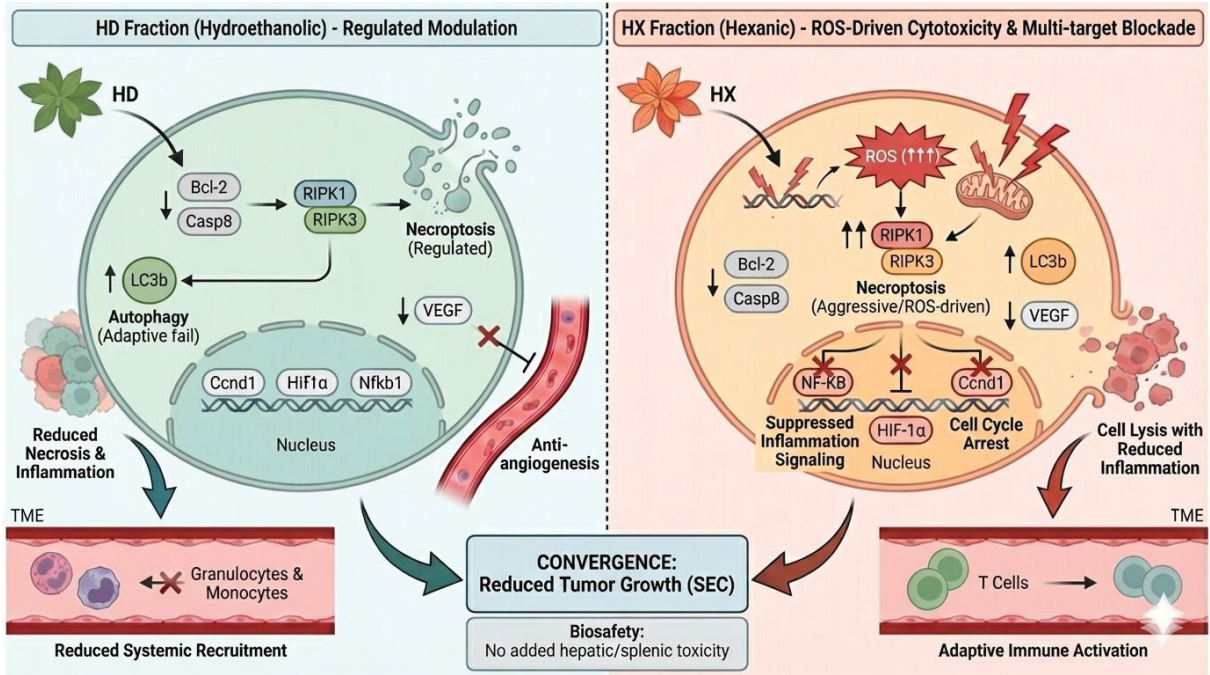
Orcid: <https://orcid.org/0000-0003-3977-687X>

Abstract

Background: *Pereskia grandifolia* is a source of food containing proteins, fibers, vitamins and minerals, and its leaves demonstrated antitumor, antioxidant and anti-inflammatory activities. It has potential for novel anticancer strategies against breast tumors. **Methods:** This study evaluated the antitumor activity of hydroethanolic (HD) and hexane (HX) fractions obtained from the leaves of *P. grandifolia* integrating *in vitro* (MCF-7 cells) and *in vivo* (Ehrlich tumor) analyses. **Results:** Phytochemically, both extracts contained triterpenes/steroids, HD has coumarins and HX has flavonoids and tannins. In MCF-7 cells HX showed strong cytotoxicity ($IC_{50} = 37 \mu\text{g}\cdot\text{mL}^{-1}$), while HD exerted a potent antiproliferative effect ($IC_{50} = 56 \mu\text{g}\cdot\text{mL}^{-1}$). Notably, both extracts abolished clonogenic survival. In female mice, HD ($100 \text{ mg}\cdot\text{kg}^{-1}$, p.o./21 days) and HX ($50 \text{ mg}\cdot\text{kg}^{-1}$, p.o./21 days) inhibited tumor progression of Solid Ehrlich Carcinoma model, but not the Ehrlich Ascitic form. Mechanistic analyses revealed a shared ability to induce programmed necroptosis (*Ripk1*, *Ripk3*, *Cas8*), autophagy (*Lc3b*), and to reduce *Vegf*, even with distinct strategies. HX acted as a cytotoxic agent, inducing ROS, and reducing the expression of genes related to inflammation (*Nfkb1*) and the cell cycle (*Ccnd1*) in tumor tissue. HD reduced necrosis and inflammatory infiltration, but modulated the systemic immunity, evidenced by decreased blood monocytes and granulocytes, while HX selectively increased lymphocytes. **Conclusion:** This study provides strong evidence that *P. grandifolia* holds multiple antitumor activities with a promising *in vivo* safety profile. These features position *P. grandifolia* as a source of anticancer compounds and support further studies aimed at developing synergistic therapeutic strategies.

Keywords: Phytochemicals, Plant extracts, Cancer murine models, Anticancer, Gene expression, Immunity

Graphical Abstract



1 INTRODUCTION

Pereskia grandifolia Haw. (Cactaceae), popularly known as “ora-pro-nóbis,” is recognized as source of food containing proteins, fibers, vitamins (A, B, and C) and minerals (Ca, Zn and Fe). These bioactive compounds render this plant a significant contributor to mitigating protein and micronutrient deficiencies (Almeida et al., 2014, Silveira et al., 2020). The amino acid profile is mainly constituted of leucine, lysine and phenylalanine (Silveira et al., 2020). Also, *P. grandifolia* has been used for centuries for its multiple therapeutic effects. In Malaysia, for instance, it is used to treat various diseases, including cancer, diabetes, hypertension, and inflammatory and rheumatic conditions (Albuquerque et al., 2025). In recent years, growing scientific evidence has confirmed several of these traditional claims, showing that *P. grandifolia* leaf extracts possess marked antioxidant, antimicrobial, cytotoxic, diuretic, and hepatoprotective properties (De Castro Campos Pinto & Scio, 2014; Rodrigues Albuquerque et al., 2023; Teixeira et al., 2023). The scientific rationale for those traditional uses is supported by evidence that the plant is a rich source of bioactive compounds such as saponins, phenolic compounds, phytosterols and alkaloids (Sim et al., 2010; Oliveira et al., 2025). Recent phytochemical analyses have also identified flavonoids such as quercetin and kaempferol derivatives, as well as triterpenes, carotenoids, and polysaccharides (Silveira et al., 2020; Teixeira et al., 2023; Lima et al., 2025). Although the exact phytochemical composition varies significantly according to the extraction method, the presence of key classes like triterpenes and phenolic compounds supports the investigation of the antitumor potential of this species, given their established cytotoxic, anti-inflammatory, and immunomodulatory activities (Vukovic et al., 2018).

Specifically, in oncology, the first study assessing the cytotoxic activity of *P. grandifolia* against breast cancer (BC) cells demonstrated in vitro cytotoxic effects in the hexane and ethyl acetate fractions (Nurestri et al., 2009). BC remains one of the most prevalent and complex malignancies worldwide, accounting for more than 2 million cases in 2022, which probably will reach 3.36 million new cases in 2045 (Bray et al., 2024). Due to its biological/ molecular complexity, BC represents a heterogeneous group of tumors and one of the most widely used classifications considers three receptors: estrogen receptor alpha (ER α), progesterone receptor (PR), and human epidermal growth factor receptor 2 (HER2) (Barzaman et al., 2020;

Lüönd et al., 2021). Among these, hormone receptor-positive tumors comprise approximately 70% of all cases and are generally associated with better clinical outcomes (Howlader et al., 2018; Li et al., 2022). However, therapeutic resistance and high recurrence rates remain major challenges in the effective management of this subtype (Andrijauskaite and Wargovich, 2022). The search for BC novel therapeutic strategies is driven not only by treatment resistance but also by the significant adverse effects associated with conventional therapies. Chemotherapeutic agents, such as taxanes and platinum derivatives often induce dose-limiting toxicities, including common and severe issues like peripheral neuropathy and immune-related adverse events. (Burstein et al., 2025; Dalferth et al., 2025).

In this context, natural products have emerged as a promising source of bioactive compounds with antitumor properties and improved safety profiles (Khan et al., 2022; Noel et al., 2020; Sayed et al., 2025). Considering the widespread traditional use of *P. grandifolia*, this study tested the hypothesis that its extracts possess antineoplastic activity against models of hormone receptor-positive breast cancer. To this end, two distinct extracts, namely hydroethanolic-soluble fraction (HD) and hexane fraction (HX), were prepared and evaluated in preclinical models of breast cancer, including *in vitro* assays using MCF-7 cells and *in vivo* employing Ehrlich carcinoma cells. Possible mechanisms of action related to oxidative stress, inflammation, cell proliferation, and cell death pathways were also investigated.

2 MATERIAL AND METHODS

2.1 CHEMICALS AND REAGENTS

RPMI 1640 medium, Fetal bovine serum (FBS) and Penicillin/Streptomycin were obtained from Gibco (ThermoFisher Scientific, Grand Island, NY, USA). Paraformaldehyde (PFA) (4%), Crystal violet, Glacial acetic acid and Trypsin/EDTA solution were sourced from ThermoFisher Scientific (Waltham, MA, USA). Bovine serum albumin, 5,5'-Dithiobis-(2-nitrobenzoic acid), Resazurin, Reduced glutathione, Xylenol orange, Butylated hydroxytoluene (BHT), Dibasic potassium phosphate, Monobasic potassium phosphate, 1 M Tris, Ethylenediaminetetraacetic acid (EDTA), Bradford Protein Assay, Tris HCl, p-Nitrofenol, Tetramethylbenzidine, Dimethylsulfoxide, Glycine, N-acetyl-beta-D-glucosamine (NAG), 2',7'-Dichlorofluorescein diacetate (DCFH-DA), Hydrochloric Acid (HCL) and N,N-dimethylformamide (DMF) were purchased from Sigma-Aldrich (St. Louis, MO, USA).

Trypan blue, Pyrogallol, Ethanol, Methanol, Ferrous ammonium sulfate, Hydrogen peroxide, Trichloroacetic acid, Formaldehyde, Citric acid, Sodium acetate, Sodium chloride, Potassium chloride, Sodium phosphate, Dibasic sodium phosphate, Hematoxylin, Eosin, Tween 20, Sulfuric acid, and Triton X-100 were obtained from Vetec (Rio de Janeiro, RJ, Brazil). Alanine aminotransaminase (ALT), Aspartate aminotransaminase (AST), Creatinine, and Total protein assays kits were acquired from Labtest (Lagoa Santa, MG, Brazil). Tumor necrosis factor α (TNF- α) and Interleukin-1 β (IL-1 β) kits were acquired from BioLegend (San Diego, CA, USA). TriZol™ reagent and Primers were obtained from Invitrogen-ThermoFisher Scientific (Waltham, MA, USA). The High-Capacity cDNA Reverse Transcription Kit and the SYBR™ Green Universal PCR Master Mix were obtained from Applied Biosystems-ThermoFisher Scientific (Waltham, MA, USA).

2.2 PLANT MATERIAL AND EXTRACTION

The leaves of *P. grandifolia* were collected in June 2021 from the Medicinal Plants Garden of Paranaense University (UNIPAR), located at an altitude of 430 m (S23°46'11.3"–W53°16'41.2"). A voucher specimen (n° 142) was deposited in the UNIPAR herbarium, and the project was registered at SISGEN (n° AD2CAC3). The plant material was oven-dried and ground. The ethanol-soluble extract was prepared by infusion, in which 100 g of powdered leaves were infused with 1 L of boiling water. The resulting infusion was stored in an amber container for 5 h and subsequently filtered. The filtrate was then treated with 95% ethanol at a 1:3 (v/v) ratio to precipitate proteins and polysaccharides. The heterogeneous phase formed was removed by filtration, and the hydroethanolic-soluble fraction (HD) was concentrated under reduced pressure using a rotary evaporator and subsequently lyophilized.

For the hexane fraction (HX), 50 g of powder were macerated in 70% ethanol for 48 h with daily solvent renewal. The extracts were filtered, concentrated under reduced pressure using a rotary evaporator, and subsequently frozen and lyophilized to obtain the crude hydroethanolic extract. This extract was dissolved in methanol–water (1:1) and subjected to liquid–liquid partitioning with hexane (3 \times). The hexane phase was collected, concentrated under reduced pressure, and lyophilized to obtain the HX fraction.

2.3 PHYTOCHEMICAL CHARACTERIZATION

A preliminary phytochemical screening was performed to qualitatively identify major classes of secondary metabolites in the HD and HX, according to Moreira (1979) and adapted by Miguel (2003). The chemical groups evaluated were alkaloids, flavonoids, coumarins, steroids, and triterpenes. For alkaloids evaluation the extracts were dissolved in ethanol and 1% HCl and tested with the general alkaloid reagents Mayer (potassium tetraiodomercurate), Dragendorff (potassium tetraiodobismuthate), and Bouchardat (iodine–potassium iodide). Positive reactions were indicated by white, brick-red, or orange precipitates, respectively. The Shinoda test was carried out to identify the flavonoids, by adding magnesium turnings and concentrated hydrochloric acid to ethanolic extracts under cooling. A pink coloration was considered a positive reaction for flavonoids. Subsequently, both HD and HX were acidified (pH 1.0 with concentrated HCl) and partitioned with ethyl ether, evaporated, and treated with NaOH (1N). The development of blue or yellow-green fluorescence under UV light at 366 nm confirmed the presence of coumarins.

For the identification of steroids and triterpenes two assays were applied: (i) Liebermann–Burchard reaction, where extracts dissolved in chloroform were treated with acetic anhydride and concentrated H_2SO_4 . Pink/blue, green, or yellow colorations indicated distinct substituents in the steroid/triterpene nucleus; (ii) Keller–Killiani reaction, in which samples dissolved in glacial acetic acid with $FeCl_3$ were layered with concentrated H_2SO_4 . A blue or green coloration at the interface indicated the presence of deoxy-sugars in steroids or triterpenes, respectively.

Finally, thin-layer chromatography (TLC) was performed. Samples were dissolved in methanol ($1\text{ mg}\cdot\text{mL}^{-1}$) and applied into silica gel 60 UV_{254} plates (Whatman®, $20 \times 20\text{ cm}$) using glass capillaries. Plates were developed with specific mobile phases and subsequently visualized under visible and UV light (254 nm). After development, the plates were sprayed with appropriate detection reagents. The metabolites screened (steroids/triterpenes, flavonoids, tannins, alkaloids and coumarins), mobile phase systems, and detection reagents are summarized in supplementary Table S1.

2.4 NUCLEAR MAGNETIC RESONANCE SPECTROSCOPIC ANALYSIS OF THE HX EXTRACT

The hexane fraction (HX) was analyzed by proton and carbon nuclear magnetic resonance spectroscopy (^1H and ^{13}C NMR). The spectra were recorded on a Bruker® AVANCE III 600 MHz TCI 5 mm N_2 Prodigy spectrometer equipped with a 14.1 T magnet, at 70 °C. The HX sample was dissolved in deuterated chloroform (CDCl_3) for spectral acquisition. Chemical shifts (δ) are expressed in parts per million (ppm), using tetramethylsilane (TMS) as the internal reference.

2.5 *IN VITRO* BREAST CANCER ASSAYS WITH MCF-7 CELLS

2.5.1 Cell Viability and Proliferation

Cell viability and proliferation were assessed sequentially in MCF-7 cells. Cells were seeded in 96-well plates at 0.5×10^4 cells/well in RPMI 1640 supplemented with 10% FBS and 1% penicillin/streptomycin, and incubated at 37 °C, 5% CO_2 , and 90% humidity for 24 h. For the viability assay, cells were treated with the compounds at 12.5, 25, 50, 100, or 200 $\mu\text{g}\cdot\text{mL}^{-1}$ for 24, 48, or 72 h. After treatment, the medium was replaced with 100 μL of 10% resazurin solution in serum-free RPMI and incubated for 3.5 h. Absorbance was measured at 570 and 595 nm using a microplate reader (Tecan Infinite M200; Tecan Group Ltd., Männedorf, Switzerland).

For the proliferation assay, wells were washed with 200 μL PBS, fixed with 100 μL of 4% paraformaldehyde for 10 min, and permeabilized with 100 μL of 2% methanol for 10 min. Cells were then stained with 80 μL of crystal violet solution for 10 min, washed thoroughly to remove excess dye, and the dye was eluted with 100 μL glacial acetic acid (33%). Proliferation was quantified by measuring absorbance at 570 nm in the same microplate reader.

2.5.2 Clonogenic Test

MCF-7 cells were seeded in 24-well plates at 5×10^2 cells/well in RPMI 1640 supplemented with 50% FBS and 1% penicillin/streptomycin, and incubated at 37 °C, 5% CO_2 , and 90% humidity for 24 h. Cells were then treated with each compound at its respective IC_{50} concentration for 72 h. After treatment, the medium containing the compound was removed, and cells were incubated with fresh culture medium for 10 days until visible colonies were formed. The medium was then removed, and cells

were fixed with 4% paraformaldehyde and stained with crystal violet, following the same procedure used in the proliferation assay, but without eluting the dye. Wells were washed thoroughly, photographed using a magnifying lens, and the number of colonies were quantified using ImageJ.

2.6 *IN VIVO* EHRLICH TUMOR MODELS

All experiments were approved by the Ethics Committee on Animal Experimentation (CEUA/BIO, UFPR, no. 1614) and followed the international guidelines for the use of animals in research (ARRIVE 2.0, Percie Du Sert et al., 2020). Specifically, adherence to the ARRIVE guidelines ensured the rigorous reporting of animal details, adherence to the 3Rs principle (Reduction), and the implementation of randomization methods in the assignment of animals to experimental groups, minimizing the risk of bias. Female Swiss mice (25–30 g) were obtained from the animal facility of the Federal University of Paraná and housed under controlled temperature (22 ± 1 °C) with a 12/12h light/dark cycle, with food and water available *ad libitum*. Environmental enrichment was provided in the cages throughout the experimental protocol.

Ehrlich tumor cells were maintained in frozen stocks at -80 °C, in culture medium supplemented with 10% DMSO + 90% fetal bovine serum, and subsequently propagated through intraperitoneal passages by inoculating 2×10^6 cells per animal. After the growth period, cells were collected in 1 mL of phosphate-buffered saline (PBS; 16.5 mM phosphate, 137 mM NaCl, and 2.7 mM KCl, pH 7.4) supplemented with 0.5 M EDTA (pH 8.0). After 3-4 passages, cell viability was assessed by the trypan blue exclusion method using a Neubauer chamber. When viability reached 95%, 2×10^6 cells were inoculated intraperitoneally to induce Ehrlich ascitic tumor, or subcutaneously into the femoral region of the right hind paw of mice, to induce the Ehrlich solid carcinoma, as described in the next sections.

2.6.1 Ascitic Ehrlich Tumor in Mice

Prior to each administration, the HD extract was dissolved in saline, and the HX fraction was dissolved in saline containing 10% Tween 20. Dose selection was guided by preclinical evidence (Rodrigues Albuquerque et al., 2023) and internal data. The hydroethanolic fraction dose corresponded to the Optimized Effective Dose (OED) identified in a pilot study. For the hexane fraction, an intermediate dose

between the minimum and optimal ranges of the HD fraction was chosen to cautiously evaluate its bioactive potential.

Mice were intraperitoneally inoculated with 2×10^6 Ehrlich tumor cells, and oral treatments commenced the following day. Animals were randomly assigned to three groups (n=5-7): Control (Ctrl), treated with saline and 10% Tween 20; HD, treated with the hydroethanolic fraction of *P. grandifolia* at $100 \text{ mg} \cdot \text{kg}^{-1}$; and HX, treated with the hexane fraction of *P. grandifolia* at $50 \text{ mg} \cdot \text{kg}^{-1}$. Treatments were administered daily by oral gavage for seven days. Body weights were recorded daily, and on the last day, the animals underwent anesthesia with isoflurane (Syntec, Tamboré, SP, Brazil) followed of euthanasia. Ascitic fluid was collected for the measurement of total volume present in the cavity and for tumor cell counting (Fig 4A).

2.6.2 Solid Ehrlich Carcinoma in Mice

Tumor-bearing mice were divided into groups of 10–12 animals: negative control (Ctrl; treated with saline and 10% Tween 20), HD (treated with HD at $100 \text{ mg} \cdot \text{kg}^{-1}$), and HX (treated with HX at $50 \text{ mg} \cdot \text{kg}^{-1}$). The preparation of extracts, vehicle composition, and dose selection followed the same protocol described for the ascitic Ehrlich tumor model. Treatments were administered orally by gavage from the first day after tumor inoculation until day 21. A naïve group of non-tumor-bearing mice was also included in the experiment.

From day 11 after inoculation, tumor volume was measured using a digital caliper (FELSEN, Wenzhou, China) by recording the largest (*L*) and smallest (*W*) tumor diameters. Tumor volume (*V*) was calculated using the formula (Mishra et al., 2018):

$$V(\text{mm}^3) = L \times W^2 \times 0.52$$

Body weight was also monitored throughout the experiment. On day 21, mice were fasted for 12h with free access to water and in the following day were anesthetized with isoflurane (Syntec, Tamboré, SP, Brazil). Blood was collected from the inferior cava vein, for biochemical and hematological analyses. After, a deeper inhalatory anesthesia induced the euthanasia. Fragments of tumor and organs, such as liver and spleen, were harvested and fixed in formalin and embedded in

histological cassettes, while the remaining samples were rapidly frozen in liquid nitrogen and stored at $-80\text{ }^{\circ}\text{C}$ for further analyses (Fig 5A).

2.7 HISTOLOGY OF TUMOR AND ORGANS

Following euthanasia, fragments of tumor, liver and spleen were immediately immersed in 10% neutral-buffered formalin at room temperature for 24–48 h. The tissues were then dehydrated in 70% ethanol and subsequently embedded in paraffin. Sections were obtained, displayed in slides and stained with hematoxylin and eosin (H&E). Histological evaluation was performed blindly by a veterinary pathologist. Histological tumor features included the necrotic area, number of macrophages, cell edema, invaded lymphatic vessels and capillaries, cells in mitoses and nuclear alterations.

2.8 OXIDATIVE STRESS PARAMETERS IN TUMOR TISSUE

Tumor samples were initially homogenized in phosphate buffer (pH 6.5). The pure homogenate was used immediately for Reduced Glutathione (GSH) determination, assessed by the method of Sedlak & Lindsay (1968) with readings at 415 nm and expressed as μg of GSH·g of tissue⁻¹. The remaining homogenate was centrifuged at 9700 rpm for 20 min, and the supernatant was diluted 1:10 in phosphate buffer for assessing the other parameters. All readings were performed using a 96-well microplate reader (Synergy HT, BioTek, VT, USA). Reactive Oxygen Species (ROS) levels were assessed based on the oxidation of dichlorodihydrofluorescein (Keston & Brandt, 1965), with fluorescence measured at 485 nm (Excitation) and 528 nm (Emission). Lipid Peroxidation (LPO) was directly measured according to the method by Jiang et al. (1992); absorbance was recorded at 560 nm, and levels were expressed as $\text{nmol}\cdot\text{min}^{-1}\cdot\text{mg protein}^{-1}$. Superoxide Dismutase (SOD) activity was measured by its ability to inhibit pyrogallol autoxidation at 440 nm (Gao et al., 1998), with enzymatic activity expressed as SOD units·mg of protein⁻¹. Finally, protein concentration was determined using the method described by Bradford (1976), with absorbance measured at 595 nm and concentration expressed in $\text{mg}\cdot\text{mL}^{-1}$.

2.9 INFLAMMATORY PARAMETERS IN TUMOR TISSUE

The levels of pro-inflammatory cytokines were measured in the supernatant of homogenized tumor tissue, obtained using the same centrifugation and dilution

protocol applied for the oxidative stress assays. Tumor necrosis factor- α (TNF- α) and interleukin-1 β (IL-1 β) concentrations were quantified using enzyme-linked immunosorbent assay (ELISA) kits (BioLegend, San Diego, CA, USA), according to the manufacturer's protocol. Additionally, macrophage infiltration in the tumor was assessed by measuring the levels of the enzyme N-acetylglucosaminidase (NAG), according to the methodology described by Bailey (1988). The assay was performed using tumor tissue samples, and absorbance was measured at 405 nm. Results were expressed as $\mu\text{mol}\cdot\text{g tissue}^{-1}$.

2.10 QUANTITATIVE REAL-TIME PCR AND BIOINFORMATICS

Total RNA was extracted from tumor tissues using the TriZol™ reagent (Invitrogen, USA) after tissue disruption by maceration in liquid nitrogen. Approximately 1 μg of RNA was reverse-transcribed into complementary DNA (cDNA) using the High-Capacity cDNA Reverse Transcription Kit (ThermoFisher Scientific, USA), following the manufacturer's protocol. The resulting cDNA was used as a template for quantitative real-time PCR (RT-qPCR) to assess relative mRNA expression levels of the target genes.

Amplification reactions were performed using SYBR™ Green Universal PCR Master Mix (Applied Biosystems, USA) in a StepOnePlus™ Real-Time PCR System (Applied Biosystems, USA). The *Rplp0* gene was used as an endogenous reference for normalization of the other genes: *Bcl-2*, *Casp8*, *Lc3b*, *Ripk1*, *Ripk3*, *Nfkb1*, *Ccnd1*, *Hif1a* and *Vegf*. The primers sequence is showed in the supplementary table S2. The assay was optimized using a 1:5 cDNA dilution factor and primer concentrations of 900 nM, ensuring amplification efficiencies between 90% and 110%. Relative gene expression levels were calculated using the $2^{-\Delta\Delta\text{CT}}$ method (Livak & Schmittgen, 2001).

To complement the gene expression analysis a bioinformatic tool was used. Protein-protein interaction (PPI) networks were constructed using the STRING database (version 12.0; <https://string-db.org>). The analysis was performed using the "Multiple Proteins by Names/Identifiers" option, with *Homo sapiens* selected as the reference organism. PPI networks were generated based on genes whose expression in Ehrlich tumor samples was significantly altered by the treatments. STRING integrates both direct (physical) and indirect (functional) associations,

derived from computational predictions, curated knowledge from primary databases, and functional inference.

2.11 BIOCHEMICAL AND HEMATOLOGICAL ASSAYS

At the end of the experiment, blood was collected using heparinized syringes for biochemical and hematological analyses. After the hemogram, the samples were centrifuged at 4000 rpm for 5 min to obtain plasma, which was used to determine ALT, AST, creatinine, and total protein levels, measured by specific kits (Labtest, Lagoa Santa, MG, Brazil) with an automated system (Cobas Mira, Roche Diagnostics, Penzberg, Germany).

2.12 DATA ANALYSIS

Data were analyzed using GraphPad Prism 9.0 software and expressed as mean \pm standard error of the mean (SEM). Differences between groups were assessed by one- or two-way analysis of variance (ANOVA), followed by Dunnett's, Bonferroni's or Tuckey post hoc test, when applicable. A p value < 0.05 was considered statistically significant. IC_{50} values were calculated using RStudio software.

3 RESULTS

3.1 PHYTOCHEMICAL SCREENING AND THIN-LAYER CHROMATOGRAPHY (TLC) SHOWED DIFFERENT COMPOUNDS IN HD AND HX

Phytochemical screening of the HD revealed the presence of flavonic heterosides, coumarins, and steroids/triterpenes, while only steroids/triterpenes were detected in the hexane fraction (Table 1). In contrast, TLC analysis revealed the presence of steroids/triterpenes and tannins in the HX fraction, whereas only steroids/triterpenes were detected in the crude HD extract under the tested conditions (Supplem. Table S3). These discrepancies likely reflect differences in the sensitivity and specificity of the two methods. Taken together, the findings suggest that the HD contains a broader phytochemical profile including coumarins, flavonoids and triterpenes/steroids, whereas the HX is enriched in triterpenes/steroids and tannins, highlighting the complementary nature of these approaches. Interestingly, none of the extracts contained alkaloids.

Table 1. Phytochemical screening for the presence of alkaloids, flavonoids, coumarins, steroids, and/or triterpenes of *P. grandifolia* extracts.

| PHYTOCHEMICAL GROUP | ANALYSIS | HD FRACTION | HX FRACTION |
|----------------------|--------------------------|-------------|-------------|
| Alkaloids | Mayer Reagent | - | - |
| | Dragendorff Reagent | - | - |
| | Bouchardat Reactive | - | - |
| Flavonic heterosides | Flavonoids | + | - |
| | Oxalic acid – Boric acid | - | - |
| Coumarins | Not applicable | + | - |
| Steroids/triterpenes | Liebermann Bouchard | + | + |
| | Keller Kelliani | + | + |

3.2 STRUCTURAL IDENTIFICATION BY NMR

NMR analyses were performed only on the hexane fraction (HX), due to its chemical profile and suitability for structural characterization. The ¹³C spectrum exhibited several signals in the region between $\delta 10$ and $\delta 50$ (Fig. 1A), which are typical of saturated carbons in aliphatic chains. Furthermore, several signals were observed in the region between $\delta 60$ and $\delta 80$, suggesting the presence of oxygen-bearing carbons. The multiplicity of these signals was confirmed by the DEPT 135 spectrum (Fig. 1B) (Machado et al., 1992). The NMR analysis of the HX revealed long-chain hydrocarbons, suggestive of triterpenes/steroids, which corroborates the findings of the phytochemical screening (Tab. 1, Supplem. Table S3).

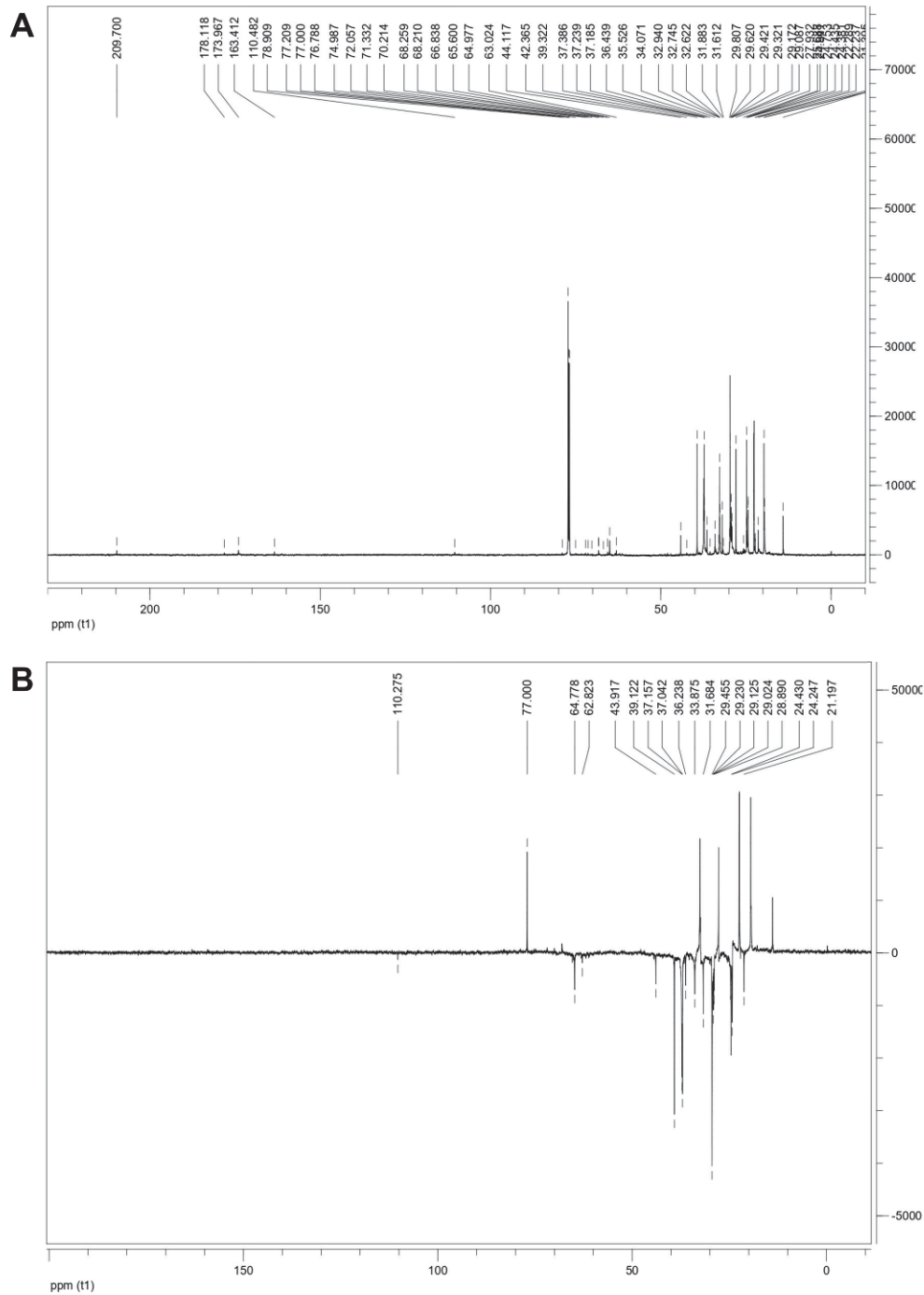


Figure 1. ^{13}C NMR Spectrum (Panel A) and DEPT 135 NMR Spectrum of the Hexane Fraction (HX) (Panel B) of *P. grandifolia*.

3.3 HX DEMONSTRATES POTENT CYTOTOXICITY AND HD A GREATER ANTIPROLIFERATIVE ACTIVITY IN MCF-7 CELLS

As illustrated in Figure 2, the analysis after 72 hours revealed distinct activity profiles for the extracts. HD reduced cell viability (Panel A) with an IC_{50} of $107 \mu\text{g}\cdot\text{mL}^{-1}$ (Pseudo- $R^2 = 0.9913$). Notably, its antiproliferative effect (Panel B) was

considerably more potent, showing an IC_{50} of $56 \mu\text{g}\cdot\text{mL}^{-1}$ (Pseudo- $R^2 = 0.9598$), with significant inhibition at all tested concentrations. In contrast, HX demonstrated marked cytotoxicity (Panel C), with an IC_{50} of $37 \mu\text{g}\cdot\text{mL}^{-1}$ (Pseudo- $R^2 = 0.9902$). However, its antiproliferative activity (Panel D) was less pronounced, with an IC_{50} of $74 \mu\text{g}\cdot\text{mL}^{-1}$ (Pseudo- $R^2 = 0.9189$). In summary, the HX fraction acted predominantly through acute cytotoxicity, while the HD extract showed a more specific and superior efficacy as an inhibitor of cell proliferation.

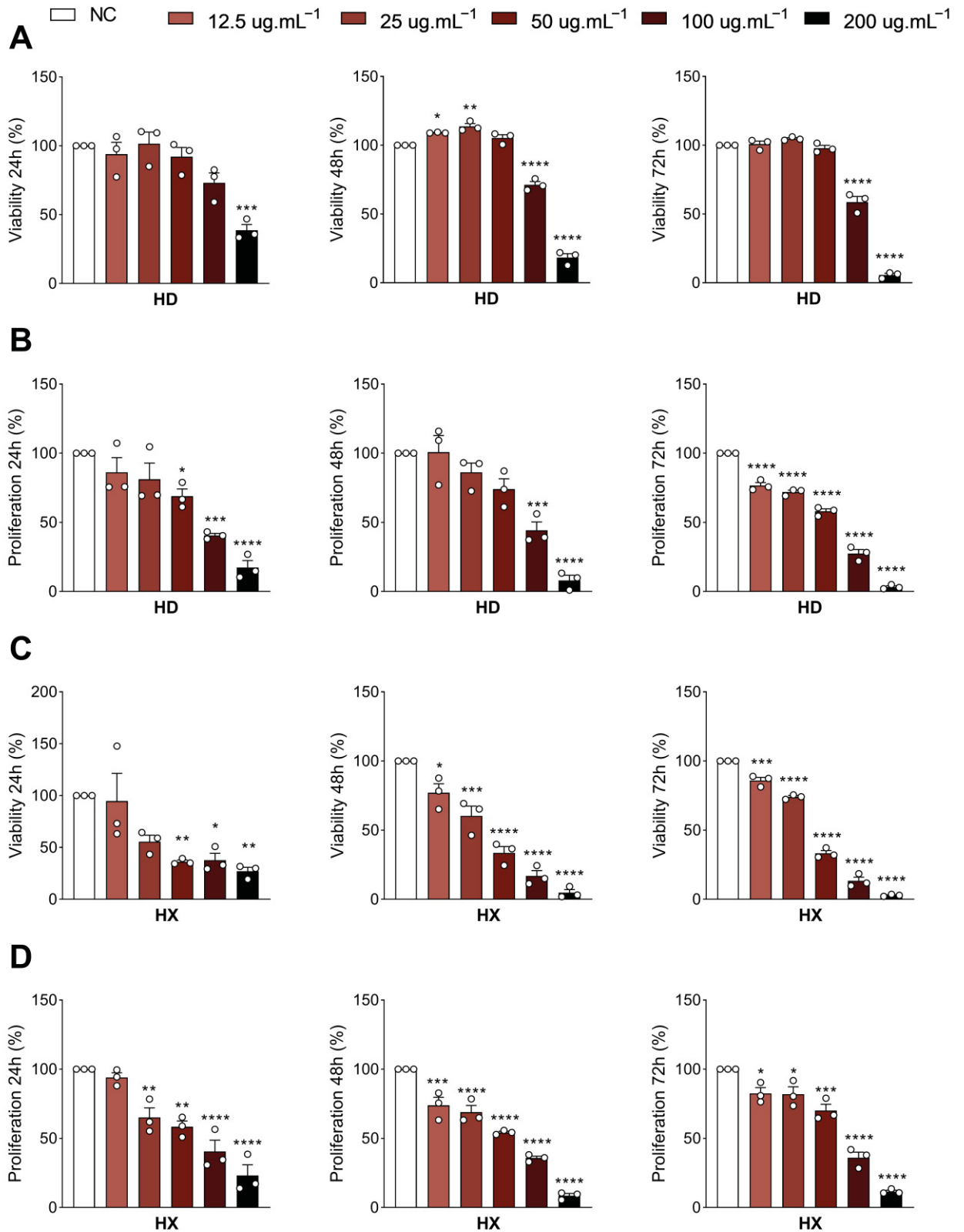


Figure 2. Effect of *Pereskia grandifolia* fractions treatment on MCF-7 cells. Panel A: Cell viability of HD at 24, 48, and 72 h. Panel B: Cell proliferation of HD at 24, 48, and 72 h. Panel C: Cell viability of HX at 24, 48, and 72 h. Panel D: Cell proliferation of HX at 24, 48, and 72 h. Data are expressed as mean \pm SEM of experiments performed in triplicate. Comparisons among groups were performed using one-way ANOVA followed by Dunnett's post hoc test. * $p < 0.05$, ** $p < 0.01$, *** $p < 0.001$, **** $p < 0.0001$.

0.0001 compared with the NC. NC, negative control; HD, hydroethanolic fraction of *P. grandifolia*; HX, hexane fraction of *P. grandifolia*.

3.4 HX AND HD REDUCE CLONOGENIC SURVIVAL OF MCF-7 CELLS

To evaluate the clonogenic potential, MCF-7 cells were treated with HD or HX extracts at their respective antiproliferative IC₅₀ concentrations. As shown in Figure 3, both extracts significantly reduced colony formation, with inhibition rates of 26.2% for HD and 21% for HX.

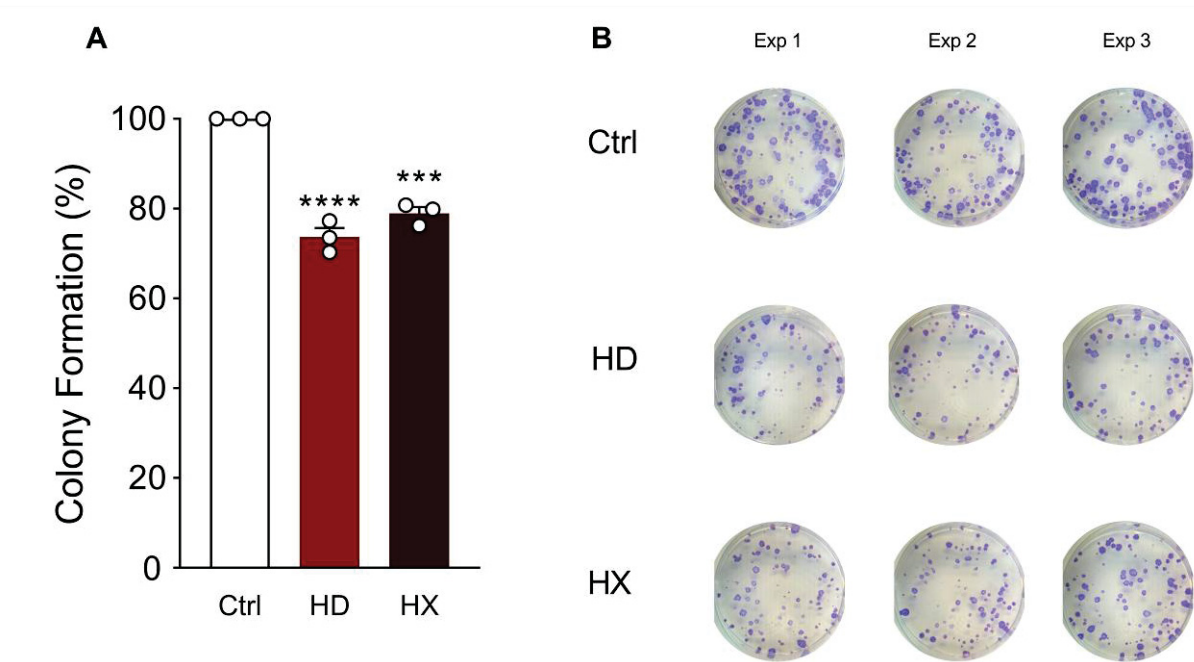


Figure 3. Clonogenic assay in MCF7 cells. Panel A: Percentage of colony formation. Panel B: Representative images. Data are expressed as mean \pm SEM of experiments performed in triplicate. Comparisons among groups were performed using one-way ANOVA followed by Dunnett's post hoc test. *** $p < 0.001$ and **** $p < 0.0001$ compared with the negative control (NC). NC, negative control; HD, hydroethanolic fraction of *P. grandifolia* ($56 \mu\text{g}\cdot\text{mL}^{-1}$); HX, hexane fraction of *P. grandifolia* ($74 \mu\text{g}\cdot\text{mL}^{-1}$).

3.5 HD AND HX DO NOT AFFECT ASCITIC TUMOR DEVELOPMENT

In the ascitic Ehrlich tumor, seven-days treatment with HD or HX did not reduce either the number of viable Ehrlich tumor cells or the tumor volume compared to the control group, indicating that short-term administration of these extracts does not affect ascitic tumor growth (Fig. 4B, C).

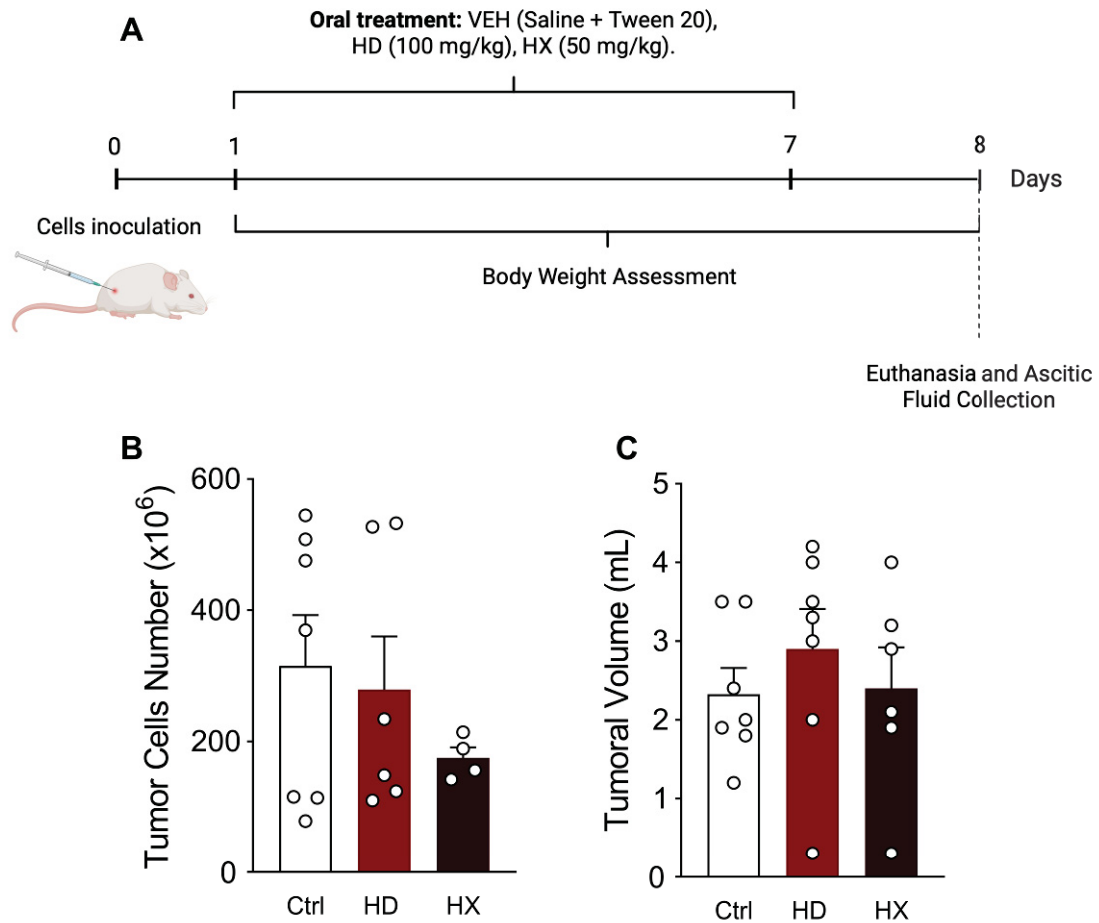


Figure 4. Effects of *P. grandifolia* extracts on ascitic Ehrlich tumor development. Panel A: Experimental design. Panel B: Number of viable tumor cells. Panel C: Total ascitic volume. Data are expressed as mean \pm SEM ($n = 5-7/\text{group}$) and analyzed by one-way ANOVA followed by Bonferroni's post hoc test. Ctrl, negative control; HD, hydroethanolic fraction of *P. grandifolia*; HX, hexane fraction of *P. grandifolia*.

3.6 HD AND HX SUPPRESS SOLID EHRlich TUMOR GROWTH

Tumor outgrowth became evident by day 11 following Ehrlich cells inoculation. Sustained administration of both extracts elicited a marked suppression of tumor progression, as reflected by significant reductions in tumor volume and weight in the treated groups compared with the control (Fig. 5B, C). By the end of the treatment period, tumor growth inhibition reached 86% and 89% in the HD- and HX-treated groups, respectively (Fig. 5D)

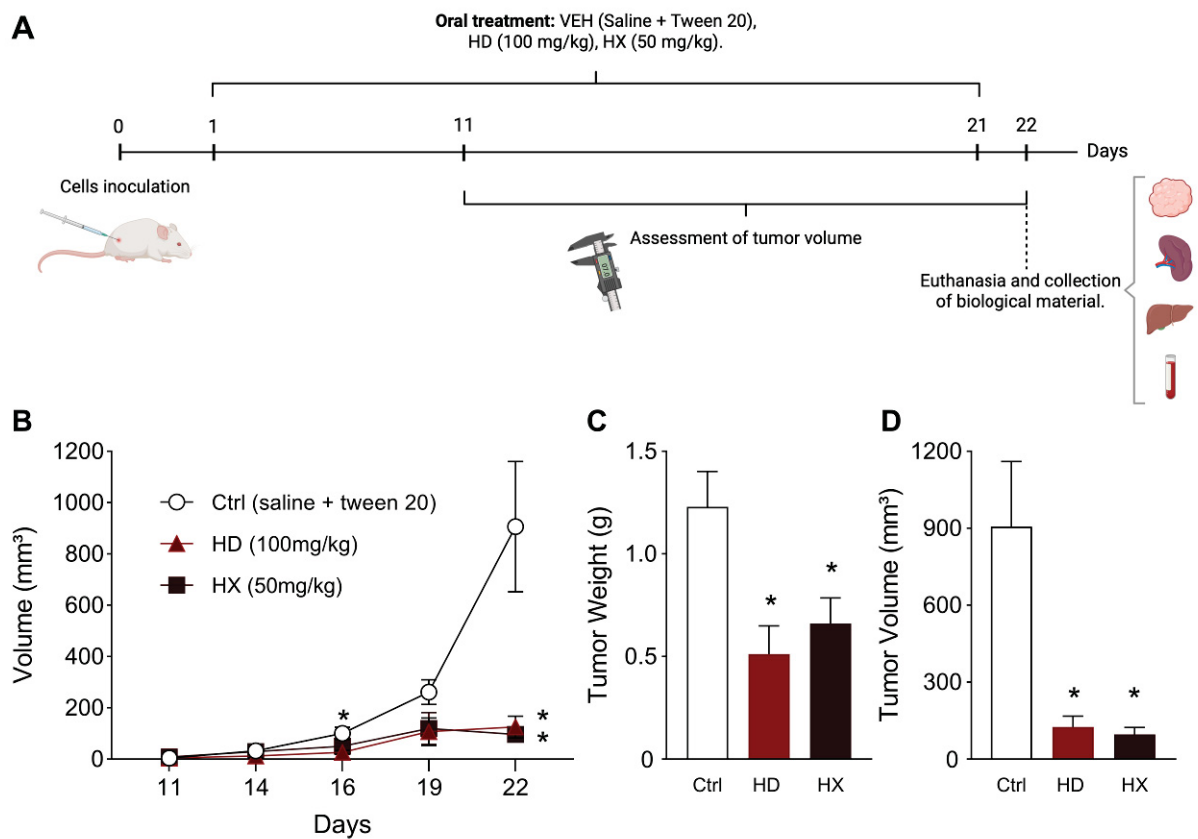


Figure 5. Experimental design and effects of *P. grandifolia* on the solid Ehrlich tumor development. Panel A: Experimental design. Panel B: Tumor growth over the 21 days of treatment. Panel C: Tumor weight at the final day. Panel D: Tumor volume at the final day. Data are expressed as mean \pm SEM ($n = 10\text{--}12/\text{group}$) and analyzed by two-way (B) or one-way ANOVA (C, D) followed by Bonferroni's post hoc test. * $p < 0.05$ compared with the Ctrl group. Ctrl, negative control; HD, hydroethanolic fraction of *P. grandifolia*; HX, hexane fraction of *P. grandifolia*.

3.7 HD AND HX INDUCED CHANGES IN TUMOR HISTOLOGY

Long-term treatment with HD significantly reduced the percentage of tumor necrotic area compared to the control group (Fig. 6B), as confirmed by quantitative morphometric analysis and the semiquantitative scoring (Fig. 6D). In contrast, HX treatment did not alter necrosis scores, which remained similar to the control (Fig. 6C). Both HD and HX treatments markedly reduced inflammatory cell infiltration (Fig. 6D), suggesting that these extracts may attenuate the proinflammatory tumor microenvironment. No significant differences were observed in apoptotic cell number, blood vessel morphology, infiltrated neutrophils, cell edema, mitotic figures, or nuclear alterations such as karyolysis and pyknosis (data not shown).

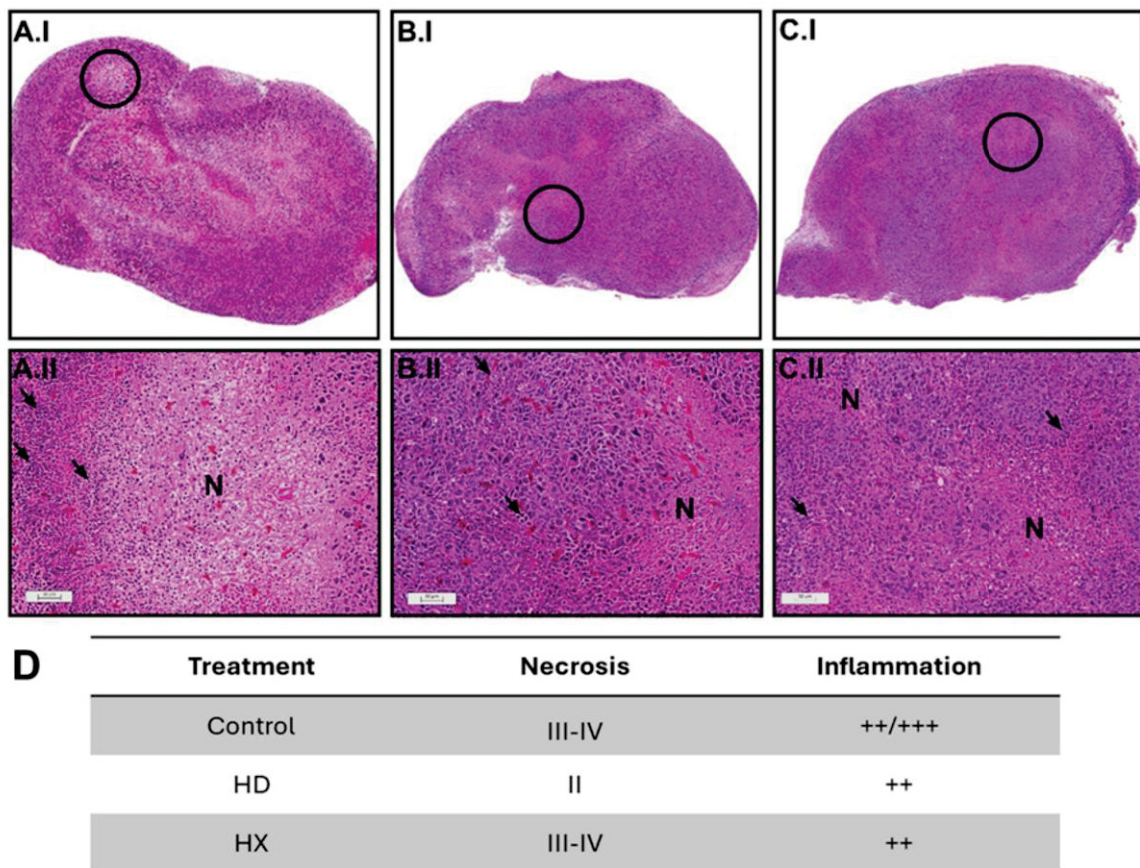


Figure 6. Histopathological analysis of tumor tissue. Representative photomicrographs of solid Ehrlich tumor sections stained with hematoxylin and eosin. (A) Control group; (B) HD group (hydroethanolic fraction of *P. grandifolia*); (C) HX group (hexane fraction of *P. grandifolia*). Panels I show the general morphology of the tumor tissue, with circles indicating the regions magnified in panels II. Panels II show necrotic areas (N) and inflammatory cells infiltration (arrows). (D) Degree of necrosis [0 (lesions <5% of the tissue), Grade I (5–25%), Grade II (26–50%), Grade III (51–75%), and Grade IV (>75%)] and inflammation [negative (-), mild (+), mild to moderate (++) , moderate (+++), and marked (++++)]. Scale bar = 50 μ m.

3.8 HX INDUCES OXIDATIVE STRESS, BUT NEITHER EXTRACTS ALTER TUMOR INFLAMMATORY PARAMETERS

In tumor tissues, HX treatment significantly increased ROS levels (Fig. 7A) and GSH levels (Fig. 7E), while showing a trend toward reduced SOD activity ($p = 0.0624$; Fig. 7C). Protein content and LPO levels remained unchanged. No relevant alterations were observed in the HD-treated group in comparison with the other treatments. Also, no significant differences in inflammatory markers (TNF- α , IL-1 β , NAG and MPO) were observed following treatment with either the HD or HX extracts (Supplem. Fig. S1).

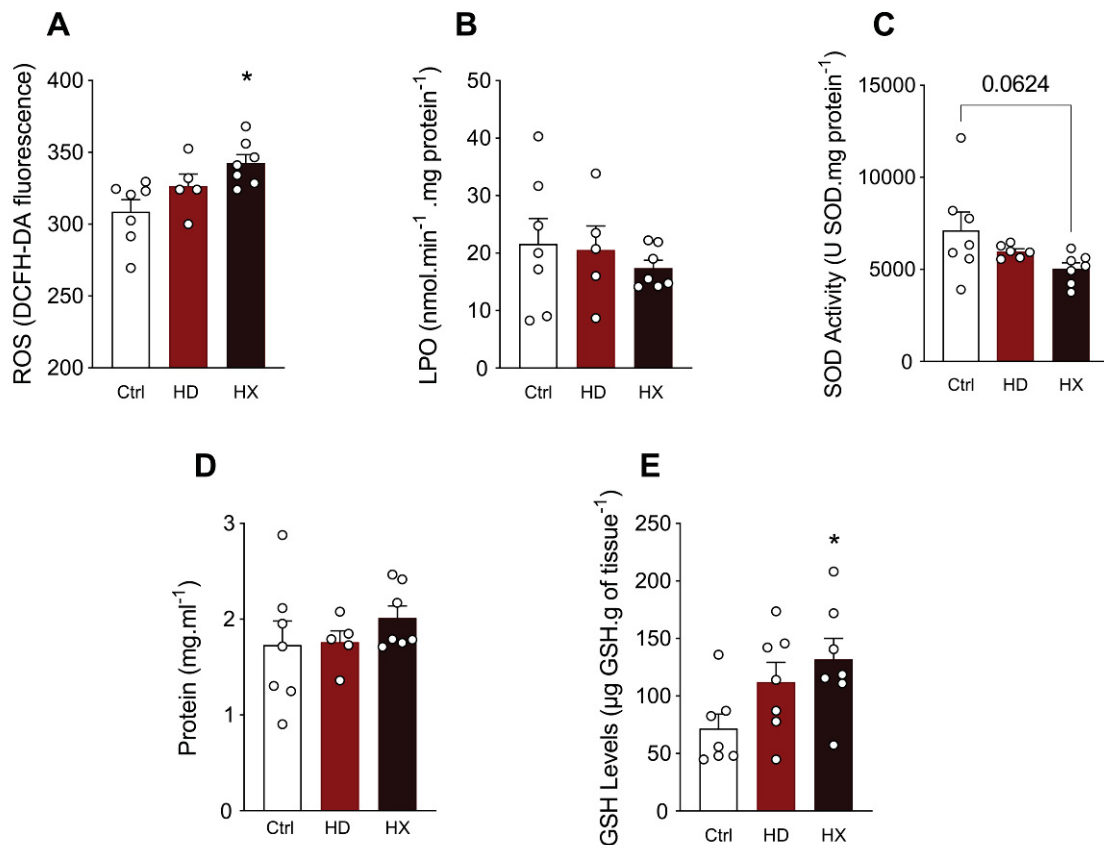


Figure 7. Oxidative stress parameters in tumor tissues. Panel A: ROS levels. Panel B: Lipid peroxidation (LPO) levels. Panel C: Superoxide dismutase (SOD) activity. Panel D: Protein concentration. Panel E: Reduced glutathione (GSH) levels. Data are expressed as mean \pm SEM ($n = 5-7$ /group) and analyzed by one-way ANOVA followed by Bonferroni's post hoc test. * $p < 0.05$ compared with the Ctrl group. Ctrl, negative control; HD, hydroethanolic fraction of *P. grandifolia*; HX, hexane fraction of *P. grandifolia*.

3.9 HD AND HX INDUCE *RIPK1/RIPK3*-MEDIATED NECROPTOSIS AND SUPPRESS SURVIVAL/PROLIFERATION PATHWAYS

Analysis of apoptotic markers revealed that both HD and HX extracts significantly reduced the expression of the anti-apoptotic gene *Bcl-2*. A pronounced effect was observed on the necroptosis pathway markers, since both extracts induced an increase in *Ripk1* and *Ripk3* expression, and a decrease in *Casp8*. Regarding autophagy, both HD and HX extracts significantly increased *Lc3b* expression. Markers associated with cell survival, proliferation, and hypoxia/angiogenesis were generally downregulated. The HX fraction significantly reduced the expression of *Nfkb1*, *Ccnd1* and *Hif1 α* , whereas both treatments decreased *Vegf* expression (Fig. 8A-I). Furthermore, the genes interaction in these

cellular pathways was corroborated by the PPI network analysis performed using the STRING tool. The main genes identified for each extract in the modulation of apoptosis, necroptosis, and autophagy pathways are biologically connected (Fig. 8J, K).

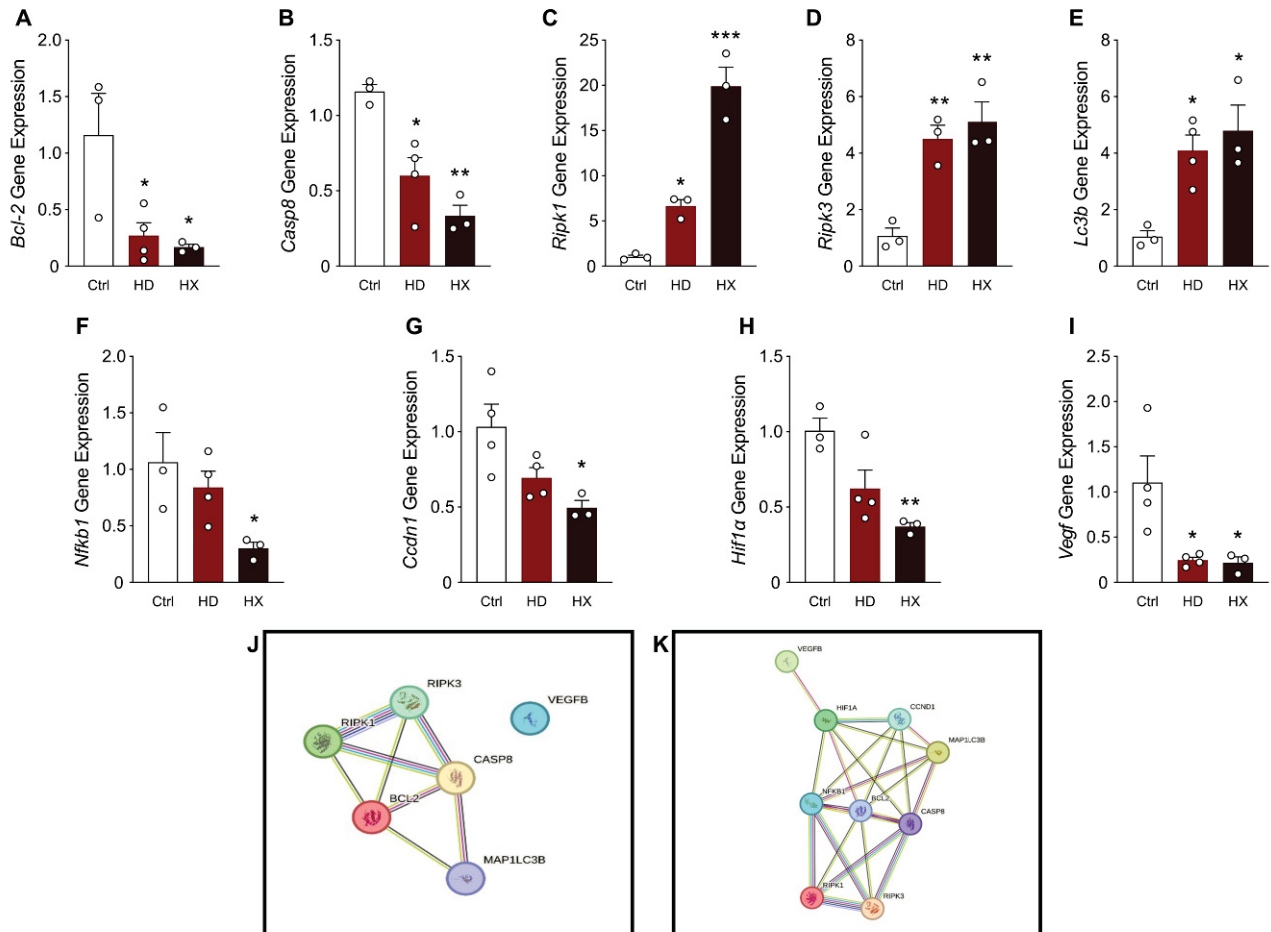


Figure 8. Effects of *P. grandifolia* extracts on expression of genes related to cell death, inflammation, proliferation, and angiogenesis in solid Ehrlich carcinoma. Relative gene expression of (A) *Bcl-2*, (B) *Casp8*, (C) *Ripk1*, (D) *Ripk3*, (E) *Lc3b*, (F) *Nfkb1*, (G) *Ccnd1*, (H) *Hif1a* and (I) *Vegf*. The proteins network from genes altered by HD (J) and HX (K) treatment is shown. Data from A to I are normalized by the *Rplp0* gene, expressed as mean \pm SEM ($n = 3-4$ /group) and analyzed by one-way ANOVA followed by Tukey's post hoc test. * $p < 0.05$, ** $p < 0.01$, and *** $p < 0.001$ compared with the Ctrl group. Ctrl: negative control; HD: hydroethanolic fraction of *P. grandifolia*; HX: hexane fraction of *P. grandifolia*. In Panels J and K the nodes represent genes, and colored edges indicate the type of interaction. Source: <https://string-db.org>

3.10 HD AND HX DID NOT INDUCE SYSTEMIC TOXICITY

Hematological and biochemical evaluations, in addition to analysis of organs involved in metabolism and immune response, were performed as indicators of

systemic toxicity of the extracts. The Ehrlich tumor development induced an increase in absolute liver and spleen weights in all tumor-bearing mice compared with naive (Table 2). Treatment with either HD or HX did not significantly change this parameter, suggesting no hepatosplenic toxicity *per se*. Instead, the organ alterations were caused by the solid tumor. In accordance, histopathological analyses (Supplem. Fig. S2) revealed similar mild hepatic alterations across all groups.

Table 2 summarizes the hematological and biochemical parameters assessed in Ehrlich tumor-bearing mice. The vehicle group exhibited increased AST, total protein, monocytes, and granulocytes, clearly related with the tumor growth when compared with the naive mice. Treatment with HD in tumor-bearing mice reduced creatinine levels as well as the total number of monocytes and granulocytes, whereas HX increased the total lymphocyte count. These hematological changes brought the values of the treated groups closer to those of the naive group, reinforcing the absence of toxicity. Other hematological indexes, including hemoglobin, hematocrit, platelets, red blood cells, and total leukocytes, showed no significant alterations among groups.

Table 2. Hematological and biochemical parameters of Ehrlich carcinoma-bearing mice treated with vehicle or *P. grandifolia* fractions and naïve mice.

| Parameter | Experimental group | | | |
|-----------------------------------|--------------------|----------------------------|--------------------------|--------------------------|
| | Nv | Ctrl | HD | HX |
| Liver weight (g) | 1.23 ± 0.07 | 1.78 ± 0.08 [#] | 1.55 ± 0.10 [#] | 1.61 ± 0.04 [#] |
| Spleen weight (g) | 0.15 ± 0.01 | 0.30 ± 0.02 [#] | 0.24 ± 0.02 [#] | 0.23 ± 0.01 [#] |
| ALT (U·L ⁻¹) | 41.68 ± 2.32 | 40.35 ± 1.95 | 42.52 ± 4.40 | 37.86 ± 1.90 |
| AST (U·L ⁻¹) | 93.44 ± 7.62 | 422.7 ± 88.33 [#] | 244.9 ± 28.55 | 290.9 ± 41.51 |
| Creatinine (mg·dL ⁻¹) | 0.55 ± 0.02 | 0.49 ± 0.01 | 0.46 ± 0.02 [#] | 0.50 ± 0.00 |

| | | | | |
|---|---------------|--------------------------|---------------|---------------|
| Total proteins (mg·dL ⁻¹) | 5.24 ± 0.17 | 5.85 ± 0.12 [#] | 5.49 ± 0.18 | 5.54 ± 0.10 |
| HBG (g·dL ⁻¹) | 12.39 ± 0.88 | 11.78 ± 0.32 | 11.42 ± 0.74 | 12.52 ± 0.40 |
| HCT (%) | 41.73 ± 2.71 | 39.01 ± 0.81 | 37.93 ± 2.23 | 42.45 ± 1.36 |
| PLT (×10 ³ ·μl ⁻¹) | 435.1 ± 29.45 | 453.4 ± 30.14 | 468.0 ± 21.87 | 508.4 ± 36.22 |
| RBC (×10 ⁶ ·μl ⁻¹) | 8.90 ± 0.55 | 8.66 ± 0.18 | 8.32 ± 0.47 | 9.29 ± 0.31 |
| WBC (×10 ³ ·μl ⁻¹) | 8.25 ± 1.17 | 8.60 ± 0.55 | 7.14 ± 0.67 | 8.47 ± 0.58 |
| Lymph (×10 ³ ·μl ⁻¹) | 6.48 ± 0.94 | 4.73 ± 0.37 | 4.13 ± 0.36 | 6.95 ± 0.81* |
| Mon (×10 ³ ·μl ⁻¹) | 0.24 ± 0.05 | 0.49 ± 0.08 [#] | 0.22 ± 0.01* | 0.35 ± 0.03 |
| Gran (×10 ³ ·μl ⁻¹) | 1.52 ± 0.20 | 3.39 ± 0.40 [#] | 1.76 ± 0.21* | 2.60 ± 0.31 |

Data are expressed as mean ± SEM (n = 7-12/group) and analyzed by one-way ANOVA followed by Bonferroni's post hoc test. **p* < 0.05 compared with the Ctrl group. [#]*p* < 0.05 compared with the Nv group. Nv: naïve group; Ctrl: negative control; HD: hydroethanolic fraction of *P. grandifolia*; HX: hexane fraction of *P. grandifolia*; HBG: hemoglobin; HCT: hematocrit; PLT: platelet; RBC: red blood cells; WBC: white blood cells; Lymph: lymphocytes; Mon: monocytes; Gran: granulocytes.

4 DISCUSSION

The present study demonstrates that the hexanic (HX) and hydroethanolic (HD) fractions of *Pereskia grandifolia* Haw. possess robust antitumoral activity against breast cancer models, despite they appear to operate via distinct and complementary mechanisms of action. The mechanistic difference among the extracts is initially evident from the *in vitro* results. The hexanic fraction (HX) showed higher acute potency, as indicated by its low IC₅₀, reflecting direct cytotoxicity. Previous studies have reported similar cytotoxic effects for different fractions of *P. grandifolia*, including the hexane fraction, in various tumor cell lines (e.g., KB, MCF-7, Saos-2) (Nurestri et al., 2009; Liew et al., 2012). In contrast, the HD demonstrated a

greater antiproliferative effect, what corroborates previous report showing potent antiproliferative activity of hydroalcoholic fraction of *P. grandifolia* against the leukemic cell line K562 (Massocatto et al., 2021).

The different effects found among both extracts can be due the extraction methods, and phytochemical and polarities differences. The presence of triterpenes/steroids in the non-polar HX fraction was highly suggested by the ¹³NMR spectroscopic analysis. The signal around 110 ppm is characteristic of an olefinic carbon commonly found in many plant triterpenes, while the numerous signals between 10 and 50 ppm correspond to the saturated carbons of the triterpenoid backbone (Mahato & Kundu, 1994; Camargo et al., 2022). Polar metabolites present in the HD fraction exhibit limited passive diffusion across lipid membranes and tend to interact preferentially with cell-surface receptors or extracellular signaling components. Such compounds are frequently associated with regulated anticancer mechanisms, including apoptosis induction and inhibition of cell proliferation (Talib & Mahasneh, 2010; Zhang et al., 2018). Conversely, the hexane extraction, which concentrates highly lipophilic compounds, may have enhanced cellular permeability and intensified direct damage to tumor cells, consistent with the stronger cytotoxic response observed (Huang et al., 2021; Rosa et al., 2025). These results also can explain the reduced cell reproductive potential in the clonogenic assay, explained by the dual strategy of *P. grandifolia*: the high acute cytotoxicity of HX (Nurestri et al., 2009) and the sustained antiproliferative activity of HD, which has been associated with programmed cell death in previous studies of polar extracts (Tan et al., 2005).

In female mice, both HX and HD significantly reduced the Ehrlich carcinoma development, which represents the first study to demonstrate the *in vivo* antitumor activity of *P. grandifolia* extracts. Interestingly, antitumoral efficacy was observed only in the solid tumor model (SEC), an outcome that strongly suggests that the extracts effects depend on the presence of a structured tumor microenvironment or of the long treatment (21 d). In this context, the complex structure of the SEC could favor local retention and prolonged exposure of bioactive compounds (Wu et al., 2024). In contrast, AEC cells remain suspended in a dynamic peritoneal fluid, promoting rapid molecular dispersion and reduced local drug concentration (Feitosa et al., 2021; Radulski et al., 2023). This limited efficacy upon AEC can also be due the short time of extracts treatment (7 d), or the oral route selected for extracts administration. Although intraperitoneal (IP) delivery would ensure substantially higher local drug

exposure, the oral route was prioritized due to its non-invasiveness and greater translational relevance (Bajaj & Yeo, 2011; Algahtani et al., 2021).

The high growth rate observed in the SEC generates severe cellular stress: proliferative regions rapidly exceed vascular supply, producing hypoxia and nutrient deprivation that culminate in central tumor necrosis (Lee et al., 2018). Furthermore, these necrotic cells contain internal molecules known as damage-associated molecular patterns (DAMPs). These DAMPs, normally hidden within the cell, are released upon membrane damage. This process promotes the activation of a pro-inflammatory response by triggering the innate immune system (Kono & Rock 2008; Man & Kanneganti., 2025). The subsequent results confirm the existence of distinct mechanisms of action between the two extracts. The HD extract decreased the tumor necrotic area, suggesting a more regulated mode of cell death that is less likely to cause extensive DAMP release and thus may attenuate downstream immune activation (Kono & Rock 2008). This hypothesis is consistent with the reduced inflammatory infiltrate observed in the tissue. In contrast, the HX fraction seems to induce a more aggressive form of direct cell death, which paradoxically results in reduced inflammatory infiltrate despite extensive cell lysis. This effect suggests that HX may contain bioactive compounds capable of uncoupling cell death from the inflammatory response, thereby suppressing the production of pro-inflammatory mediators (Bagherniya et al., 2021; Agrawal et al., 2025; Li et al., 2025). Together, these mechanisms could explain the absence of changes in inflammatory biomarkers (TNF- α , IL-1 β , NAG, MPO). In HD-treated tissue, this pattern is consistent with reduced inflammatory activation secondary to more controlled cell death, while in HX-treated tissue, it may reflect suppression of downstream signaling, supported by the downregulation of *Nfkb1*, a key transcription factor involved in amplifying inflammatory responses following DAMP sensing (Liu et al., 2017). This mechanistic divergence is reinforced by the distinct roles of oxidative stress. The HX fraction exerts its effects by inducing ROS, thereby causing widespread damage to DNA, proteins, and lipids, which eventually leads to cell death (Niu et al., 2021; An et al., 2024). In an attempt to resist this damage, the tumor cells activate their endogenous antioxidant systems, such as GSH and SOD (Liu et al., 2023; Brandl et al., 2025), probably overwhelming the cellular machinery and forcing a pro-oxidant state.

Despite those differences, the necroptosis pathway was activated in tumor of both extract-treated groups, as evidenced by the upregulation of *Ripk1* and *Ripk3*,

and downregulation of *Casp8* and *Bcl-2*. *Casp8* acts as a negative regulator of necroptosis, redirecting death-receptor signaling from necroptosis toward apoptosis (Ch'en et al., 2011; Weinlich & Green, 2014). Moreover, the intensity of *Ripk1* upregulation varied between extracts, being more pronounced in the HX treatment. This finding strongly corroborates the HX mechanism, as several studies have reported that *Ripk1* activation is highly sensitive to and mainly driven by ROS and cellular damage (Zhang et al., 2017; Wang et al., 2022). Furthermore, both HD and HX extracts significantly increased *Lc3b* expression, indicating stress-induced activation of autophagy (Mizushima et al., 2008). This likely represents an adaptive response that ultimately fails to counterbalance the necroptotic program triggered by *P. grandifolia* extracts. Additionally, HD and HX treatments converged in their anti-angiogenic activity, as both significantly reduced the expression of *Vegf*, and HX downregulated the hypoxia sensor *Hif1a*. The capacity of both extracts to block angiogenesis is fundamental to limit the tumor blood supply and growth potential (Goel & Mercurio, 2014), since angiogenesis inhibitors (rhuMAb VEGF or bevacizumab) have been investigated in BC therapy (Pegram et al., 2002). Finally, the HX fraction significantly reduced the expression of the cell cycle regulator *Ccnd1* (Cyclin D1). This comprehensive downregulation of proliferation and stress-adaptation genes confirms the HX role as a multi-target cytotoxic agent (Qannita et al., 2024; Mondalto & Amicis, 2020). While the HD extract did not significantly alter the expression of these genes, its efficacy is less dependent on directly shutting down these transcriptionally controlled proliferation pathways, aligning instead with its strategy of modulating the TME. Furthermore, the PPI network analysis by bioinformatic strongly reinforces these mechanistic differences.

To evaluate how these extracts act systemically, hematological analysis was performed. The HD extract-induced decrease in circulating granulocytes and monocytes reflects a potential selective action on the myeloid lineage or in their trafficking, as the absence of significant changes in other cell lineages suggests this is not a generalized myelosuppressive effect. Rather than representing an adverse effect, this response may constitute a key therapeutic mechanism: by limiting the availability of these precursor cells, the HD extract restricts their recruitment to the tumor microenvironment. This is relevant because these cells commonly differentiate into pro-tumoral phenotypes, including TAMs and myeloid-derived suppressor cells (MDSCs). MDSCs, representing neutrophil and monocyte lineages (Akkari, et al.,

2024), actively support angiogenesis, immunosuppressive activity and immune evasion (Anderson & Simon., 2021; Zhao et al., 2023). Conversely, the therapeutic efficacy of the HX fraction appears linked to the positive modulation of the adaptive immune response. An increased infiltration of T cells within the TME is frequently associated with a favorable prognosis in cancer patients (Anderson & Simon., 2021).

Crucially, no overt signs of toxicity were observed in the animals treated with either extract, as evidenced by the lack of significant changes in biochemical and hematological parameters, and the absence of morphological changes in organs analyzed. This suggests that the therapeutic effects of the HD and HX extracts are achieved without inducing severe systemic adverse effects. This finding is consistent with previous reports that have demonstrated the good safety profile of a *P. grandifolia* ethanolic-soluble fraction and methanolic extract *in vivo* (Sri Nurestri et al., 2010; Rodrigues Albuquerque et al., 2023). While the present results are promising, further long-term studies are necessary to fully assess chronic toxicity and ensure its safety for translational applications.

Despite the consistent antitumor data, this study has two main limitations: (a) qualitative analyses of the extracts were performed, without full characterization of the majority compounds present in each sample; and (b) *in vivo* experiments lacked both a standard chemotherapeutic agent (positive control), and a healthy (non-tumor bearing) group treated with the extract for a full assessment of systemic toxicity. The omission of these control groups is justified by the 3Rs principle of animal experimentation, specifically *Reduction*, and by the fact that the mechanisms and effects of clinically used chemotherapeutic agents are already well established. These limitations are the starting point for further investigations with *P. grandifolia* extracts.

In conclusion, this study provides the first *in vivo* evidence that compounds from *Pereskia grandifolia* possess significant antitumor potential, with multi-target mechanisms. These findings strongly position *P. grandifolia* as a promising source of anticancer compounds and highlight the value of combined extract-based approaches. Nevertheless, further studies are needed to identify the active molecules and clarify their mechanisms. These distinct pharmacological profiles provide a solid basis for bioactivity-guided fractionation and for assessing their translational potential.

Funding Sources

This work was supported by the Brazilian agencies Coordenação de Aperfeiçoamento de Pessoal de Nível Superior (CAPES, Financial code 001) and Conselho Nacional de Desenvolvimento Científico e Tecnológico (CNPq, Process 303600/2025-0).

Authors contribution

Gabrielle Oliveira Guilherme: Writing – original draft, Methodology, Investigation; **Suelen C.S. Baal:** Methodology, Investigation, Writing - original draft; **Cintia Aparecida dos Anjos, Obdulio Gomes Miguel, Bruna Isadora Pilger, Julia Helena Carvalho, André Felipe Naidek, Luana Eloisa Leal, Kauê Marcel Oliveira, Gabriela Casani Cardoso, Jaqueline Carvalho de Oliveira, Francislaine Aparecida dos Reis Lívero, Gustavo Ratti da Silva, Edneia Amancio de Souza Ramos,** Methodology, Investigation; **Maria Carolina Stipp:** Methodology, Writing – review & editing; **Alexandra Acco:** Writing – review & editing, Project administration, Funding acquisition, Conceptualization.

Declaration of Competing Interest

The authors do not have any competing interest.

Acknowledgements

The authors thank Dr. Elisiane de Bona Sartor, Dr. Marilis Dallarmi Miguel, Dr. Arquimedes Santana Filho, Dr. Guilherme Lanzi Sassaki, and Dr. Claudia Martins Galindo for their help with the experiments; and Centro de Tecnologias Avançadas em Fluorescência (CTAF-UFPR) and the NMR Center – UFPR for technical support.

Data availability

Data will be made available on request.

Declaration of generative AI use

The authors confirm the use of AI tools for language editing, using online DeepL and ChatGPT.

5 REFERENCES

Agrawal, S., Narang, S., Shahi, Y., & Mukherjee, S. (2025). Inhibitors of inflammasome (NLRP3) signaling pathway as promising therapeutic candidates for oral cancer. *Biochimica et Biophysica Acta (BBA) - General Subjects*, 1869(6), 130800. <https://doi.org/10.1016/j.bbagen.2025.130800>

Albuquerque, E. R., Braga, F. D. A., Martins, G. B., Silva, E. P., Negrini, K. S., Yoshitani, C. M. E., Kluck, A. J., Garnier, L. P., Silva, G. R. D., Ribeiro-Paes, J. T., & Lívero, F. A. D. R. (2025). Exploring the Biomedical Potential of *Pereskia grandifolia*: A Comprehensive Review of Botanical, Phytochemical, and Pharmacological Aspects. *Journal of Medicinal Food*, 1096620X251389604. <https://doi.org/10.1177/1096620X251389604>

Almeida, M. E. F., et al. (2014). Chemical characterization of the non-conventional vegetable known as ora-pro-nobis. *Bioscience Journal*, 30, 431–439.

An, X., Yu, W., Liu, J., Tang, D., Yang, L., & Chen, X. (2024). Oxidative cell death in cancer: Mechanisms and therapeutic opportunities. *Cell Death & Disease*, 15(8), 556. <https://doi.org/10.1038/s41419-024-06939-5>

Anderson, N. M., & Simon, M. C. (2020). The tumor microenvironment. *Current Biology*, 30(16), R921–R925. <https://doi.org/10.1016/j.cub.2020.06.081>

Andrijauskaite, K., & Wargovich, M. J. (2022). Role of natural products in breast cancer related symptomology: Targeting chronic inflammation. *Seminars in Cancer Biology*, 80, 370–378. <https://doi.org/10.1016/j.semcancer.2020.08.011>

Akkari, L., Amit, I., Bronte, V., Fridlender, Z. G., Gabrilovich, D. I., Ginhoux, F., Hedrick, C. C., & Ostrand-Rosenberg, S. (2024). Defining myeloid-derived suppressor cells. *Nature Reviews Immunology*, 24(12), 850–857. <https://doi.org/10.1038/s41577-024-01062-0>

Bailey, P. J. (1988). Sponge implants as models. *Methods in Enzymology* (V. 162, p. 327–334). Elsevier. [https://doi.org/10.1016/0076-6879\(88\)62087-8](https://doi.org/10.1016/0076-6879(88)62087-8)

Bagherniya, M., Khedmatgozar, H., Fakheran, O., Xu, S., Johnston, T. P., & Sahebkar, A. (2021). Medicinal plants and bioactive natural products as inhibitors of NLRP3 inflammasome. *Phytotherapy Research*, 35(9), 4804–4833. <https://doi.org/10.1002/ptr.7118>

Bajaj, G., & Yeo, Y. (2010). Drug Delivery Systems for Intraperitoneal Therapy. *Pharmaceutical Research*, 27(5), 735–738. <https://doi.org/10.1007/s11095-009-0031-z>

Bradford, M. M. (1976). A rapid and sensitive method for the quantitation of microgram quantities of protein utilizing the principle of protein-dye binding. *Analytical Biochemistry*, 72(1–2), 248–254. [https://doi.org/10.1016/0003-2697\(76\)90527-3](https://doi.org/10.1016/0003-2697(76)90527-3)

Brandl, N., Seitz, R., Sendtner, N., Müller, M., & Gülow, K. (2025). Living on the Edge: ROS Homeostasis in Cancer Cells and Its Potential as a Therapeutic Target. *Antioxidants*, 14(8), 1002. <https://doi.org/10.3390/antiox14081002>

Bray, F., Laversanne, M., Sung, H., Ferlay, J., Siegel, R.L., Soerjomataram, I., Jemal, A. (2024). Global Cancer Statistics 2022: GLOBOCAN Estimates of Incidence and Mortality Worldwide for 36 Cancers in 185 Countries. *CA Cancer J Clin*, 74, 229–263. doi:10.3322/caac.21834

Burstein, H. J., Curigliano, G., Gnant, M., Loibl, S., Regan, M. M., Loi, S., Denkert, C., Poortmans, P., Cameron, D., Thurlimann, B., Weber, W. P., Aebi, S., Al-Foheidi, M., Bago-Horvath, Z., Bidard, F.-C., Boughey, J., Morales, D. B., Brucker, S., Burstein, H. J., ... Yin, Y. (2025). Tailoring treatment to cancer risk and patient preference: The 2025 St Gallen International Breast Cancer Consensus Statement on individualizing therapy for patients with early breast cancer. *Annals of Oncology*, S0923753425047180. <https://doi.org/10.1016/j.annonc.2025.09.007>

Camargo, K. C., De Aguilar, M. G., Moraes, A. R. A., De Castro, R. G., Szczerbowski, D., Miguel, E. L. M., Oliveira, L. R., Sousa, G. F., Vidal, D. M., & Duarte, L. P. (2022). Pentacyclic Triterpenoids Isolated from Celastraceae: A Focus in the ¹³C-NMR Data. *Molecules*, 27(3), 959. <https://doi.org/10.3390/molecules27030959>

de Castro Campos Pinto, N., & Scio, E. (2014). The Biological Activities and Chemical Composition of *Pereskia* Species (Cactaceae)—A Review. *Plant Foods for Human Nutrition*, 69(3), 189–195. <https://doi.org/10.1007/s11130-014-0423-z>

Ch'en, I. L., Tsau, J. S., Molkenin, J. D., Komatsu, M., & Hedrick, S. M. (2011). Mechanisms of necroptosis in T cells. *Journal of Experimental Medicine*, 208(4), 633–641. <https://doi.org/10.1084/jem.20110251>

Dalferth, R., Hebbel, H., Bauerschlag, D., Letsch, A., & Schmidt, T. (2025). Effects on chemotherapy-induced peripheral neuropathy by moderate strength

training in combination with whole-body vibration in breast cancer patients. *Supportive Care in Cancer*, 33(11), 970. <https://doi.org/10.1007/s00520-025-09972-y>

Feitosa, I. B., Mori, B., Teles, C. B. G., & Costa, A. G. D. (2021). What are the immune responses during the growth of Ehrlich's tumor in ascitic and solid form? *Life Sciences*, 264, 118578. <https://doi.org/10.1016/j.lfs.2020.118578>

Gao, R., Yuan, Z., Zhao, Z., & Gao, X. (1998). Mechanism of pyrogallol autoxidation and determination of superoxide dismutase enzyme activity. *Bioelectrochemistry and Bioenergetics*, 45(1), 41–45. [https://doi.org/10.1016/S0302-4598\(98\)00072-5](https://doi.org/10.1016/S0302-4598(98)00072-5)

Goel, H. L., & Mercurio, A. M. (2013). VEGF targets the tumour cell. *Nature Reviews Cancer*, 13(12), 871–882. <https://doi.org/10.1038/nrc3627>

Howlander, N., Cronin, K. A., Kurian, A. W., & Andridge, R. (2018). Differences in Breast Cancer Survival by Molecular Subtypes in the United States. *Cancer Epidemiology, Biomarkers & Prevention*, 27(6), 619–626. <https://doi.org/10.1158/1055-9965.EPI-17-0627>

Huang, Y., Wang, J., Wang, S., Xu, X., Qin, W., Wen, Y., Zhao, Y. H., & Martyniuk, C. J. (2021). Discrimination of active and inactive substances in cytotoxicity based on Tox21 10K compound library: Structure alert and mode of action. *Toxicology*, 462, 152948. <https://doi.org/10.1016/j.tox.2021.152948>

Jiang, Z.-Y., Hunt, J. V., & Wolff, S. P. (1992). Ferrous ion oxidation in the presence of xylenol orange for detection of lipid hydroperoxide in low density lipoprotein. *Analytical Biochemistry*, 202(2), 384–389. [https://doi.org/10.1016/0003-2697\(92\)90122-N](https://doi.org/10.1016/0003-2697(92)90122-N)

Keston, A. S., & Brandt, R. (1965). The fluorometric analysis of ultramicro quantities of hydrogen peroxide. *Analytical Biochemistry*, 11(1), 1–5. [https://doi.org/10.1016/0003-2697\(65\)90034-5](https://doi.org/10.1016/0003-2697(65)90034-5)

Khan, M. I., Bouyahya, A., Hachlafi, N. E. L., Menyiy, N. E., Akram, M., Sultana, S., Zengin, G., Ponomareva, L., Shariati, M. A., Ojo, O. A., Dall'Acqua, S., & Elebiyo, T. C. (2022). Anticancer properties of medicinal plants and their bioactive compounds against breast cancer: A review on recent investigations. *Environmental Science and Pollution Research*, 29(17), 24411–24444. <https://doi.org/10.1007/s11356-021-17795-7>

Kono, H., & Rock, K. L. (2008). How dying cells alert the immune system to danger. *Nature Reviews Immunology*, 8(4), 279–289. <https://doi.org/10.1038/nri2215>

Lee, S. Y., Ju, M. K., Jeon, H. M., Jeong, E. K., Lee, Y. J., Kim, C. H., Park, H. G., Han, S. I., & Kang, H. S. (2018). Regulation of Tumor Progression by Programmed Necrosis. *Oxidative Medicine and Cellular Longevity*, 2018(1), 3537471. <https://doi.org/10.1155/2018/3537471>

Li, H., Liu, T., Shi, X., Du, H., Cai, C., Yang, D., Qu, L., Dou, H., Jiao, B., & Jiao, B. (2025). Mechanisms and therapeutic potential of pharmacological agents targeting inflammasomes. *Biomedicine & Pharmacotherapy*, 189, 118164. <https://doi.org/10.1016/j.biopha.2025.118164>

Li, Z., Wei, H., Li, S., Wu, P., & Mao, X. (2022). The Role of Progesterone Receptors in Breast Cancer. *Drug Design, Development and Therapy*, Volume 16, 305–314. <https://doi.org/10.2147/DDDT.S336643>

Liew, S.-Y., Stanbridge, E. J., Yusoff, K., & Shafee, N. (2012). Hypoxia affects cellular responses to plant extracts. *Journal of Ethnopharmacology*, 144(2), 453–456. <https://doi.org/10.1016/j.jep.2012.09.024>

Lima, J. D., Menegazzo, R. F., Silva, M. F., Barbosa, M. P. S. B., Schuelter, A. R., Jacomassi, E., & Silva, G. J. (2025). Comparative analysis of selected nutrients in *Pereskia* species. *Brazilian Journal of Biology*, 85, e290533. <https://doi.org/10.1590/1519-6984.290533>

Livak, K. J., & Schmittgen, T. D. (2001). Analysis of Relative Gene Expression Data Using Real-Time Quantitative PCR and the $2^{-\Delta\Delta CT}$ Method. *Methods*, 25(4), 402–408. <https://doi.org/10.1006/meth.2001.1262>

Liu, T., Zhang, L., Joo, D., & Sun, S.-C. (2017). NF- κ B signaling in inflammation. *Signal Transduction and Targeted Therapy*, 2(1), 17023. <https://doi.org/10.1038/sigtrans.2017.23>

Liu, Y., Shi, Y., Han, R., Liu, C., Qin, X., Li, P., & Gu, R. (2023). Signaling pathways of oxidative stress response: The potential therapeutic targets in gastric cancer. *Frontiers in Immunology*, 14, 1139589. <https://doi.org/10.3389/fimmu.2023.1139589>

Lüönd, F., Tiede, S., & Christofori, G. (2021). Breast cancer as an example of tumour heterogeneity and tumour cell plasticity during malignant progression. *British Journal of Cancer*, 125(2), 164–175. <https://doi.org/10.1038/s41416-021-01328-7>

Machado, E. C., Zanatta, N., & Morel, A. F. (1993). ATRIBUIÇÃO DOS DESLOCAMENTOS QUÍMICOS DE 1H E ^{13}C DO ALCALÓIDE CICLOPEPTÍDICO

DISCARINA-B POR TÉCNICAS DE RMN DE 1D E 2D. *Química Nova*, 16(5), 400–405.

Mahato, S. B., & Kundu, A. P. (1994). ¹³C NMR Spectra of pentacyclic triterpenoids—A compilation and some salient features. *Phytochemistry*, 37(6), 1517–1575. [https://doi.org/10.1016/S0031-9422\(00\)89569-2](https://doi.org/10.1016/S0031-9422(00)89569-2)

Man, S. M., & Kanneganti, T.-D. (2024). Innate immune sensing of cell death in disease and therapeutics. *Nature Cell Biology*, 26(9), 1420–1433. <https://doi.org/10.1038/s41556-024-01491-y>

Massocatto, A. M., Silva, N. F. D. S., Kazama, C. C., Pires, M. D. B., Takemura, O. S., Jacomassi, E., Ruiz, A. L. T. G., & Laverde Junior, A. (2021). Biological activity survey of *Pereskia aculeata* Mill. and *Pereskia grandifolia* Haw. (Cactaceae). *Pharmaceutical Sciences*, 1. <https://doi.org/10.34172/PS.2021.27>

Miguel, O. G. Ensaio sistemático de análise fitoquímica. Apostila da disciplina de fitoquímica do curso de farmácia da UFPR. Curitiba, 2003.

Mizushima, N., Levine, B., Cuervo, A. M., & Klionsky, D. J. (2008). Autophagy fights disease through cellular self-digestion. *Nature*, 451(7182), 1069–1075. <https://doi.org/10.1038/nature06639>

Moreira, E. A Marcha sistemática de análise em fitoquímica. *Tribuna farmacêutica*, v. 47, p. 1-19, 1979

Mishra, S., Tamta, A. K., Sarikhani, M., Desingu, P. A., Kizkekra, S. M., Pandit, A. S., Kumar, S., Khan, D., Raghavan, S. C., & Sundaresan, N. R. (2018). Subcutaneous Ehrlich Ascites Carcinoma mice model for studying cancer-induced cardiomyopathy. *Scientific Reports*, 8(1), 5599. <https://doi.org/10.1038/s41598-018-23669-9>

Niu, B., Liao, K., Zhou, Y., Wen, T., Quan, G., Pan, X., & Wu, C. (2021). Application of glutathione depletion in cancer therapy: Enhanced ROS-based therapy, ferroptosis, and chemotherapy. *Biomaterials*, 277, 121110. <https://doi.org/10.1016/j.biomaterials.2021.121110>

Noel, B., Singh, S. K., Lillard Jr., J. W., & Singh, R. (2020). Role of natural compounds in preventing and treating breast cancer. *Frontiers in Bioscience*, 12(1), 137–160. <https://doi.org/10.2741/S544>

Nurestri, A. M. S., Sim, K. S., & Norhanom, A. W. (2009). Phytochemical and Cytotoxic Investigations of *Pereskia grandifolia* Haw. (Cactaceae) Leaves. *Journal of Biological Sciences*, 9(5), 488–493. <https://doi.org/10.3923/jbs.2009.488.493>

Qannita, R. A., Alalami, A. I., Harb, A. A., Aleidi, S. M., Taneera, J., Abu-Gharbieh, E., El-Huneidi, W., Saleh, M. A., Alzoubi, K. H., Semreen, M. H., Hudaib, M., & Bustanji, Y. (2024). Targeting Hypoxia-Inducible Factor-1 (HIF-1) in Cancer: Emerging Therapeutic Strategies and Pathway Regulation. *Pharmaceuticals*, 17(2), 195. <https://doi.org/10.3390/ph17020195>

Oliveira, R. M., Costa, I. H. D. L., Antunes, B. D. F., Schirmann, G. D. S., Oliveira, F. M., Jansen-Alves, C., De Oliveira, E. G., & Zambiasi, R. C. (2025). Chemical composition, bioactive compounds, biological activity, and applications of ora-pro-nóbis (*Pereskia* spp.): A review. *Food Research International*, 221, 117239. <https://doi.org/10.1016/j.foodres.2025.117239>

Pegram, M.D.; Reese, D.M. Combined biological therapy of breast cancer using monoclonal antibodies directed against HER2/protein and vascular endothelial growth factor. *Semin. Oncol.* 2002, 29, 29–37

Percie Du Sert, N., Ahluwalia, A., Alam, S., Avey, M. T., Baker, M., Browne, W. J., Clark, A., Cuthill, I. C., Dirnagl, U., Emerson, M., Garner, P., Holgate, S. T., Howells, D. W., Hurst, V., Karp, N. A., Lazic, S. E., Lidster, K., MacCallum, C. J., Macleod, M., ... Würbel, H. (2020). Reporting animal research: Explanation and elaboration for the ARRIVE guidelines 2.0. *PLOS Biology*, 18(7), e3000411. <https://doi.org/10.1371/journal.pbio.3000411>

Radulski, D. R., Stipp, M. C., Galindo, C. M., & Acco, A. (2023). Features and applications of Ehrlich tumor model in cancer studies: A literature review. *Translational Breast Cancer Research*, 4, 22–22. <https://doi.org/10.21037/tbcr-23-32>

Rodrigues Albuquerque, E., Ratti Da Silva, G., De Abreu Braga, F., Pelegrini Silva, E., Sposito Negrini, K., Rodrigues Fracasso, J. A., Pires Guarnier, L., Jacomassi, E., Ribeiro-Paes, J. T., Da Silva Gomes, R., Gasparotto Junior, A., & Lívero, F. A. D. R. (2023). Bridging the Gap: Exploring the Preclinical Potential of *Pereskia grandifolia* in Metabolic-Associated Fatty Liver Disease. *Evidence-Based Complementary and Alternative Medicine*, 2023(1), 8840427. <https://doi.org/10.1155/2023/8840427>

Rosa, A., Pollastro, F., Sogos, V., & Piras, F. (2025). Comparative Evaluation of Cytotoxic and Apoptotic Effects of Natural Compounds in SH-SY5Y Neuroblastoma Cells in Relation to Their Physicochemical Properties. *Molecules*, 30(8), 1742. <https://doi.org/10.3390/molecules30081742>

Sayed, A. A., Abdullah, M. S., WalyEldeen, A. A., Sayed, R. M. S., Gabre, R. M., Ibrahim, S. A., & Hassan, H. (2025). *Cicer arietinum* extract as antitumor and protective agent against Ehrlich Solid Carcinoma-bearing mice. *BMC Complementary Medicine and Therapies*, 25(1), 325. <https://doi.org/10.1186/s12906-025-05061-z>

Sedlak, J., & Lindsay, R. H. (1968). Estimation of total, protein-bound, and nonprotein sulfhydryl groups in tissue with Ellman's reagent. *Analytical Biochemistry*, 25, 192–205. [https://doi.org/10.1016/0003-2697\(68\)90092-4](https://doi.org/10.1016/0003-2697(68)90092-4)

Silveira, M. G., Picinin, C. T. R., Cirillo, M. Â., Freire, J. M., & Barcelos, M. D. F. P. (2020). Nutritional assay *Pereskia* spp.: Unconventional vegetable. *Anais da Academia Brasileira de Ciências*, 92(suppl 1), e20180757. <https://doi.org/10.1590/0001-3765202020180757>

Sim, K. S., Sri Nurestri, A. M., & Sinniah, S. K. (2010). Phenolic content and antioxidant activity of *Pereskia grandifolia* Haw. (Cactaceae) extracts. *Pharmacognosy Magazine*, 6(23), 248–254. <https://doi.org/10.4103/0973-1296.66945>

Sri Nurestri, A., Sinniah, S., Kim, K., Norhanom, A., & Sim, K. (2010). Acute oral toxicity of *Pereskia bleo* and *Pereskia grandifolia* in mice. *Pharmacognosy Magazine*, 6(21), 67. <https://doi.org/10.4103/0973-1296.59969>

Talib, W. H. (2010). Antiproliferative Activity of Plant Extracts Used Against Cancer in Traditional Medicine. *Scientia Pharmaceutica*, 78(1), 33–45. <https://doi.org/10.3797/scipharm.0912-11>

Tan, M. L., Sulaiman, S. F., Najimuddin, N., Samian, M. R., & Muhammad, T. S. T. (2005). Methanolic extract of *Pereskia bleo* (Kunth) DC. (Cactaceae) induces apoptosis in breast carcinoma, T47-D cell line. *Journal of Ethnopharmacology*, 96(1–2), 287–294. <https://doi.org/10.1016/j.jep.2004.09.025>

Teixeira, V. M. C., Oliveira, A. D., Backes, E., Souza, C. G. M. D., Castoldi, R., Sá-Nakanishi, A. B. D., Bracht, L., Comar, J. F., Corrêa, R. C. G., Leimann, F. V., Bracht, A., & Peralta, R. M. (2023). A Critical Appraisal of the Most Recent Investigations on Ora-Pro-Nobis (*Pereskia* sp.): Economical, Botanical, Phytochemical, Nutritional, and Ethnopharmacological Aspects. *Plants*, 12(22), 3874. <https://doi.org/10.3390/plants12223874>

Vukovic, N. L., Obradovic, A. D., Vukic, M. D., Jovanovic, D., & Djurdjevic, P. M. (2018). Cytotoxic, proapoptotic and antioxidative potential of flavonoids isolated from propolis against colon (HCT-116) and breast (MDA-MB-231) cancer cell lines.

Food Research International, 106, 71–80.
<https://doi.org/10.1016/j.foodres.2017.12.056>

Wagner, H. *Plant Drugs analysis*. 2. ed. Berlin: Springer, p 298-299; 1996.

Wang, B., Fu, J., Chai, Y., Liu, Y., Chen, Y., Yin, J., Pu, Y., Chen, C., Wang, F., Liu, Z., Zheng, L., & Chen, M. (2022). Accumulation of RIPK1 into mitochondria is requisite for oxidative stress-mediated necroptosis and proliferation in Rat Schwann cells. *International Journal of Medical Sciences*, 19(13), 1965–1976.
<https://doi.org/10.7150/ijms.69992>

Weinlich, R., & Green, D. R. (2014). The Two Faces of Receptor Interacting Protein Kinase-1. *Molecular Cell*, 56(4), 469–480.
<https://doi.org/10.1016/j.molcel.2014.11.001>

Wu, B., Zhang, B., Li, B., Wu, H., & Jiang, M. (2024). Cold and hot tumors: From molecular mechanisms to targeted therapy. *Signal Transduction and Targeted Therapy*, 9(1), 274. <https://doi.org/10.1038/s41392-024-01979-x>

Zhao, Y., Du, J., & Shen, X. (2023). Targeting myeloid-derived suppressor cells in tumor immunotherapy: Current, future and beyond. *Frontiers in Immunology*, 14, 1157537. <https://doi.org/10.3389/fimmu.2023.1157537>

Zhang, H.-W., Hu, J.-J., Fu, R.-Q., Liu, X., Zhang, Y.-H., Li, J., Liu, L., Li, Y.-N., Deng, Q., Luo, Q.-S., Ouyang, Q., & Gao, N. (2018). Flavonoids inhibit cell proliferation and induce apoptosis and autophagy through downregulation of PI3K mediated PI3K/AKT/mTOR/p70S6K/ULK signaling pathway in human breast cancer cells. *Scientific Reports*, 8(1), 11255. <https://doi.org/10.1038/s41598-018-29308-7>

Zhang, Y., Su, S. S., Zhao, S., Yang, Z., Zhong, C.-Q., Chen, X., Cai, Q., Yang, Z.-H., Huang, D., Wu, R., & Han, J. (2017). RIP1 autophosphorylation is promoted by mitochondrial ROS and is essential for RIP3 recruitment into necrosome. *Nature Communications*, 8(1), 14329.
<https://doi.org/10.1038/ncomms14329>

6 SUPPLEMENTARY MATERIAL

Supplementary Table S1. Mobile phases and detection techniques used for thin-layer chromatography of *P. grandifolia* extracts.

| Metabolite | Mobile Phase | Detection Reagent | Expected Result | Reference |
|----------------------|---|-------------------------------------|---|--------------|
| Steroids/Triterpenes | Toluene: Ethyl acetate (93:7) | Vanillin–sulfuric acid (1%) | Blue-violet and/or green bands; dark brown bands (polyphenols) | Wagner, 1996 |
| Flavonoids | Ethyl acetate: Formic acid: Glacial acetic acid: Water (100:11:11:26) | NEU reagent | Green and/or orange bands; red-brown or chestnut bands under UV light (254 nm) | Wagner, 1996 |
| Tannins | Ethyl acetate: Formic acid: Glacial acetic acid: Water (100:11:11:26) | Ferric chloride (5% in ethanol) | Blue bands (hydrolysable tannins) and/or red bands (condensed tannins); dark brown to black bands (polyphenols) | Wagner, 1996 |
| Alkaloids | Chloroform: Methanol (95:5), saturated with ammonia | Dragendorff reagent | Orange bands | Wagner, 2006 |
| Coumarins | Toluene: Ethyl acetate (80:20) | NEU reagent and 1N sodium hydroxide | Blue fluorescent bands under UV (254 nm), with intensified fluorescence after NaOH | Miguel, 2003 |

NEU reagent: 1% diphenylboric acid 2-aminoethyl ester in methanol.

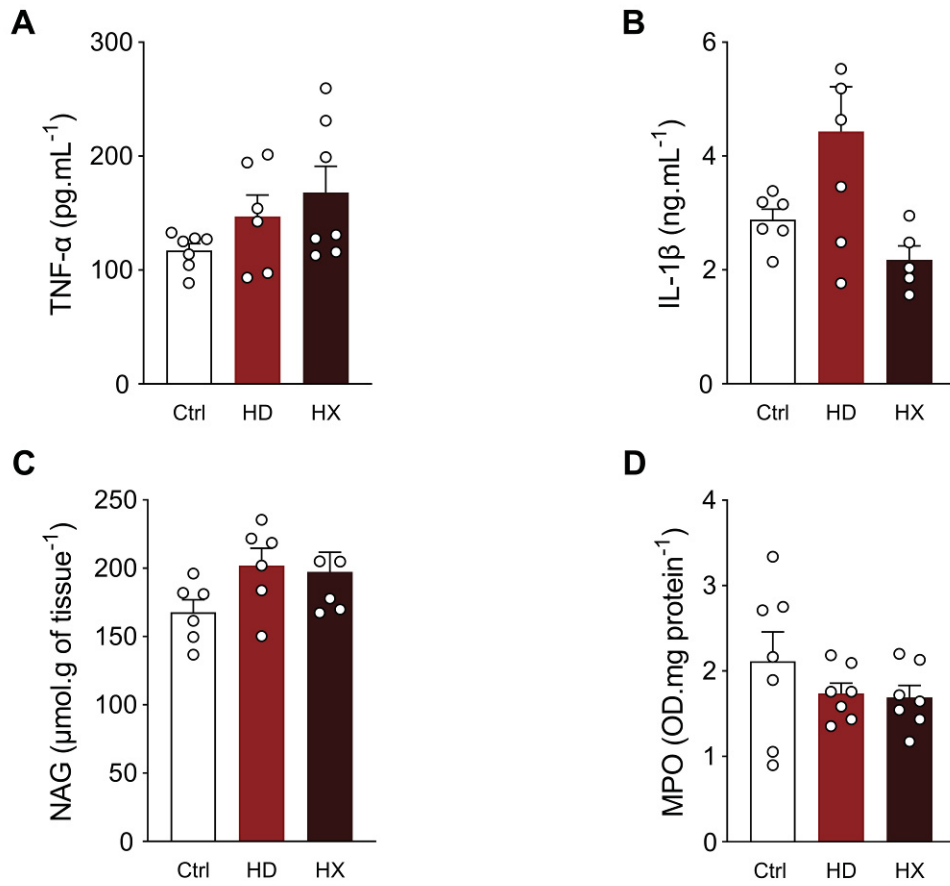
Supplementary Table S2. Primers used to perform RTqPCR in mice Ehrlich tumor samples.

| Gene | Primer (Forward) | Primer (Reverse) |
|--------------|----------------------------|------------------------------|
| <i>Rplp0</i> | 5'- TTATAACCCTGAAGTGCTCGAC | 5'- CGCTTGTACCCATTGATGATG |
| <i>Hif1a</i> | 5'- TGGATTTTGGCAGCGATGAC | 5'- TGGCTTTGGAGTTTCCGATG |
| <i>Vegf</i> | 5'- ACTGGACCCTGGCTTTACTGCT | 5'-TGATCCGCATGATCTGCATGGTG |
| <i>Bcl-2</i> | 5'- CACTTGCCACTGTAGAGA | 5'- GCTTCACTGCCTCCTT |
| <i>Ripk1</i> | 5'- TGTCTACAGCTTTGGGATCCTC | 5'- TGCCTGTCACACACTGTTTC |
| <i>Ripk3</i> | 5 - GAAGACACGGCACTCCTTGGTA | 5' - CTTGAGGCAGTAGTTCTTGGTGG |
| <i>Casp8</i> | 5'- GATCCTGTGAATGGAACCTG | 5'- CATCCTGACTGGCGTGAACCTA |
| <i>Lc3b</i> | 5'- GTCCTGGACAAGACCAAGTTCC | 5'- CCATTCACCAGGAGGAAGAAGG |
| <i>Nfkb1</i> | 5'- TGGAGGCATGTTCCGGTAGTG | 5'- TGCGTTGGATTTTCGTGACTC |

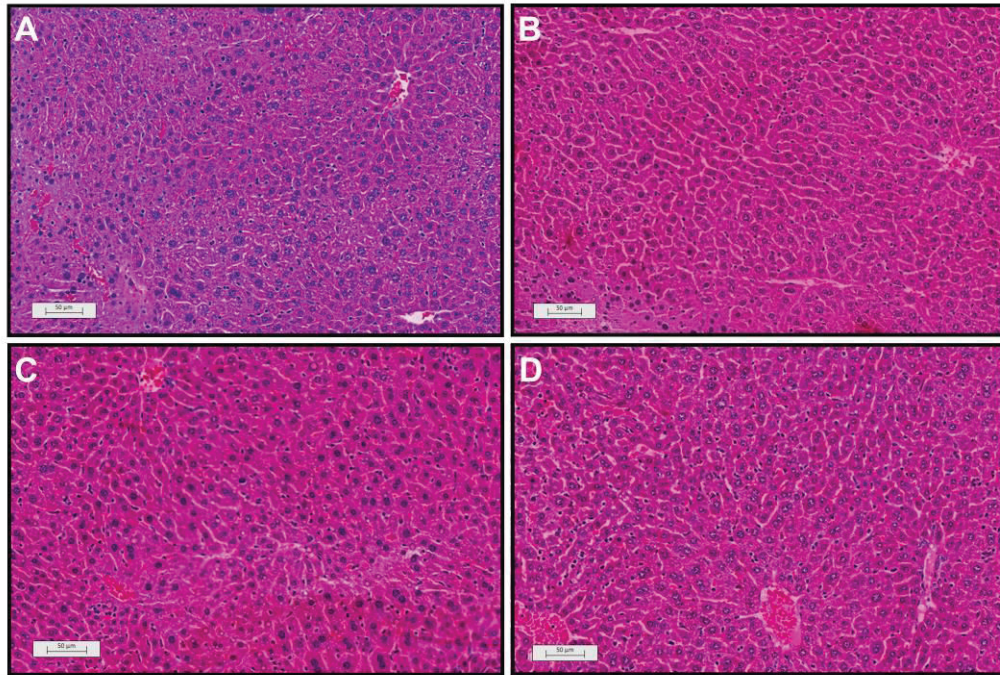
Rplp0, ribosomal protein lateral stalk subunit P0; *Hif1a*, hypoxia inducible factor 1 subunit alpha; *Vegf*, vascular endothelial growth factor; *Bcl2*, B-cell lymphoma 2; *Ripk1*, receptor-interacting serine/threonine-protein kinase 1; *Ripk3*, receptor-interacting protein kinase 3; *Casp8*, caspase-8; *Lc3b*, microtubule-associated proteins 1A/1B light chain 3B; *Nfkb1*: nuclear Factor Kappa B Subunit 1.

Supplementary Table S3. Characterization of secondary metabolites of *P. grandifolia* extracts by thin-layer chromatography (TLC) assay.

| Samples | Secondary Metabolites | | | | |
|-------------|-----------------------|------------|---------|-----------|-----------|
| | Steroids/triterpenes | Flavonoids | Tannins | Coumarins | Alkaloids |
| HD FRACTION | + | - | - | - | - |
| HX FRACTION | + | - | + | - | - |



Supplementary Figure S1. Assessment of inflammatory markers in Ehrlich solid tumor tissue. Panel A: TNF- α levels. Panel B: IL-1 β levels. Panel C: N-acetylglucosaminidase (NAG) activity. Panel D: Myeloperoxidase (MPO) activity. Data are expressed as mean \pm SEM (n = 5–7/group) and analyzed by one-way ANOVA followed by Bonferroni's post hoc test. Ctrl, negative control; HD, hydroalcoholic extract of *P. grandifolia*; HX, hexane extract of *P. grandifolia*.



Supplementary Figure S2. Representative photomicrographs of liver sections from mice bearing Ehrlich solid tumor. Panel A: Naïve group; Panel B: Negative control group; Panel C: Hydroalcoholic extract of *P. grandifolia* (HD); Panel D: Hexane extract of *P. grandifolia* (HX). Liver sections were stained with hematoxylin and eosin (H&E). Mild and similar hepatic alterations were observed among groups, characterized by diffuse congestion, discrete hepatocellular vacuolization, and mild mononuclear inflammatory infiltrate. Scale bar = 50 µm.

4. CONSIDERAÇÕES FINAIS

O presente estudo demonstrou a eficácia antitumoral das frações hexânica (HX) e hidroetanólica (HD) das folhas de *P. grandifolia* em modelos pré-clínicos de câncer de mama, especificamente no tumor sólido. A caracterização química evidenciou perfis fitoconstituintes distintos, refletindo-se na singularidade de mecanismos moleculares. Embora ambas as frações tenham convergido para a indução de morte celular por necroptose (ativação de *Ripk1/Ripk3*) e inibição da angiogênese (redução de *Vegf*), as vias de sinalização à montante diferiram substancialmente.

A fração hidroetanólica (HD) apresentou um mecanismo de ação mais regulado, associado a uma menor necrose tecidual e inflamação no microambiente tumoral. Sistemicamente, promoveu uma redução seletiva de granulócitos e monócitos circulantes, sugerindo um potencial bloqueio no recrutamento de células da linhagem mieloide que favorecem o tumor. Em contraste, a fração hexânica (HX) exibiu uma ação pleiotrópica mediada por estresse oxidativo (ROS), exacerbando a via necroptótica. Além da citotoxicidade direta, a fração HX atuou como um agente multialvo, suprimindo vias cruciais de sobrevivência, hipóxia e proliferação. No âmbito sistêmico, observou-se linfocitose, indicando uma possível estimulação da resposta imune adaptativa.

Ressalta-se que este trabalho constitui a primeira avaliação *in vivo* do potencial antitumoral da *P. grandifolia*, propondo mecanismos moleculares inéditos para sua atividade. Entretanto, algumas limitações importantes devem ser reconhecidas. A principal refere-se à ausência de uma caracterização fitoquímica quantitativa, o que impediu a correlação direta entre bioativos específicos e os achados biológicos descritos. Adicionalmente, o desenho experimental não contemplou a associação com terapias convencionais. Sendo assim, ainda se faz necessária a realização de ensaios de combinação com quimioterápicos (como doxorrubicina ou paclitaxel) para verificar a existência (ou não) de efeitos sinérgicos, visando potencializar a resposta terapêutica e mitigar efeitos colaterais. Dessa forma, investigações futuras tornam-se essenciais para preencher essas lacunas, ampliando a robustez dos dados e o entendimento sobre a aplicabilidade clínica da espécie vegetal *P. grandifolia*.

5. REFERÊNCIAS

- Aboeella, N. S., Brandle, C., Kim, T., Ding, Z.-C., & Zhou, G. (2021). Oxidative Stress in the Tumor Microenvironment and Its Relevance to Cancer Immunotherapy. *Cancers*, 13(5), 986. <https://doi.org/10.3390/cancers13050986>
- Albuquerque, E. R., Braga, F. D. A., Martins, G. B., Silva, E. P., Negrini, K. S., Yoshitani, C. M. E., Kluck, A. J., Garnier, L. P., Silva, G. R. D., Ribeiro-Paes, J. T., & Lívero, F. A. D. R. (2025). Exploring the Biomedical Potential of *Pereskia grandifolia*: A Comprehensive Review of Botanical, Phytochemical, and Pharmacological Aspects. *Journal of Medicinal Food*, 1096620X251389604. <https://doi.org/10.1177/1096620X251389604>
- Amaral, E. C., Veiga, A. D. A., Atherino, J. C., Souza, W. M. D., Kita, D. H., Lívero, F. A., Ratti, G. D. S., Rosa, S. R. B., Jacomassi, E., & Souza, L. M. D. (2025). Unveiling the Phytochemical Diversity of *Pereskia aculeata* Mill. and *Pereskia grandifolia* Haw.: An Antioxidant Investigation with a Comprehensive Phytochemical Analysis by Liquid Chromatography with High-Resolution Mass Spectrometry. *Pharmaceuticals*, 19(1), 38. <https://doi.org/10.3390/ph19010038>
- Cao, Y., Yi, Y., Han, C., & Shi, B. (2024). NF-κB signaling pathway in tumor microenvironment. *Frontiers in Immunology*, 15, 1476030. <https://doi.org/10.3389/fimmu.2024.1476030>
- Comşa, Ş., Cîmpean, A. M., & Raica, M. (2015). The Story of MCF-7 Breast Cancer Cell Line: 40 years of Experience in Research. *Anticancer Research*, 35(6), 3147–3154.
- Devaraji, M., & Thanikachalam, P. V. (2025). Phytoconstituents as emerging therapeutics for breast cancer: Mechanistic insights and clinical implications. *Cancer Pathogenesis and Therapy*, 3(5), 364–382. <https://doi.org/10.1016/j.cpt.2025.02.006>
- Drăgănescu, M., & Carmocan, C. (2017). Hormone Therapy in Breast Cancer. *Chirurgia*, 112(4), 413. <https://doi.org/10.21614/chirurgia.112.4.413>
- Dvir, K., Giordano, S., & Leone, J. P. (2024). Immunotherapy in Breast Cancer. *International Journal of Molecular Sciences*, 25(14), 7517. <https://doi.org/10.3390/ijms25147517>
- Feitosa, I. B., Mori, B., Teles, C. B. G., & Costa, A. G. D. (2021). What are the immune responses during the growth of Ehrlich's tumor in ascitic and solid form? *Life Sciences*, 264, 118578. <https://doi.org/10.1016/j.lfs.2020.118578>
- Fisher, B.; Bryant, J.; Wolmark, N.; Mamounas, E.; Brown, A.; Fisher, E.R.; Wickerham, D.L.; Begovic, M.; DeCillis, A.; Robidoux, A.; et al. Effect of preoperative chemotherapy on the outcome of women with operable breast cancer. *J. Clin. Oncol.* 1998, 16, 2672–2685.

Fisusi, F. A., & Akala, E. O. (2019). Drug Combinations in Breast Cancer Therapy. *Pharmaceutical Nanotechnology*, 7(1), 3–23. <https://doi.org/10.2174/2211738507666190122111224>

Garroni, G., Cruciani, S., Serra, D., Pala, R., Coradduzza, D., Cossu, M. L., Ginesu, G. C., Ventura, C., & Maioli, M. (2024). Effects of the MCF-7 Exhausted Medium on hADSC Behaviour. *International Journal of Molecular Sciences*, 25(13), 7026. <https://doi.org/10.3390/ijms25137026>

Hanahan, D. (2022). Hallmarks of Cancer: New Dimensions. *Cancer Discovery*, 12(1), 31–46. <https://doi.org/10.1158/2159-8290.CD-21-1059>

Instituto Nacional de Câncer (INCA). (2023). *Câncer de mama: vamos falar sobre isso?* Ministério da Saúde. https://www.inca.gov.br/sites/ufu.sti.inca.local/files/media/document/cartilha_cancer_de_mama_2022_visualizacao.pdf

Kundu, M., Butti, R., Panda, V. K., Malhotra, D., Das, S., Mitra, T., Kapse, P., Gosavi, S. W., & Kundu, G. C. (2024). Modulation of the tumor microenvironment and mechanism of immunotherapy-based drug resistance in breast cancer. *Molecular Cancer*, 23(1), 92. <https://doi.org/10.1186/s12943-024-01990-4>

Kwapisz, D. Cyclin-dependent kinase 4/6 inhibitors in breast cancer: Palbociclib, ribociclib, and abemaciclib. *Breast Cancer Res. Treat.* 2017, 166, 41–54.

Laverde Junior, A., Cavéquia, B. M., Rezende, B. H., & Rodrigues, M. V. (2022). POTENCIAL NUTRACÊUTICO DE PERESKIA GRANDIFOLIA HAW. (CACTACEAE). Em M. L. D. Miranda, *Fitoquímica: Potencialidades biológicas dos biomas brasileiros—Volume 2* (1^o ed., p. 109–127). Editora Científica Digital. <https://doi.org/10.37885/220508852>

Li, Y., Zhao, B., Peng, J., Tang, H., Wang, S., Peng, S., Ye, F., Wang, J., Ouyang, K., Li, J., Cai, M., & Chen, Y. (2024). Inhibition of NF-κB signaling unveils novel strategies to overcome drug resistance in cancers. *Drug Resistance Updates*, 73, 101042. <https://doi.org/10.1016/j.drug.2023.101042>

Loibl, S., Poortmans, P., Morrow, M., Denkert, C., & Curigliano, G. (2021). Breast cancer. *The Lancet*, 397(10286), 1750–1769. [https://doi.org/10.1016/S0140-6736\(20\)32381-3](https://doi.org/10.1016/S0140-6736(20)32381-3)

Łukasiewicz, S., Czeczelewski, M., Forma, A., Baj, J., Sitarz, R., & Stanisławek, A. (2021). Breast Cancer—Epidemiology, Risk Factors, Classification, Prognostic Markers, and Current Treatment Strategies—An Updated Review. *Cancers*, 13(17), 4287. <https://doi.org/10.3390/cancers13174287>

Lüönd, F., Tiede, S., & Christofori, G. (2021). Breast cancer as an example of tumour heterogeneity and tumour cell plasticity during malignant progression. *British Journal of Cancer*, 125(2), 164–175. <https://doi.org/10.1038/s41416-021-01328-7>

- Nurestri, A. M. S., Sim, K. S., & Norhanom, A. W. (2009). Phytochemical and Cytotoxic Investigations of *Pereskia grandifolia* Haw. (Cactaceae) Leaves. *Journal of Biological Sciences*, 9(5), 488–493. <https://doi.org/10.3923/jbs.2009.488.493>
- Orrantia-Borunda, E., Anchondo-Nuñez, P., Acuña-Aguilar, L. E., Gómez-Valles, F. O., & Ramírez-Valdespino, C. A. (2022). Subtypes of Breast Cancer. Em Department of Medical Education, Dr. Kiran C. Patel College of Allopathic Medicine, Nova Southeastern University, FL, USA & H. N. Mayrovitz (Org.), *Breast Cancer* (p. 31–42). Exon Publications. <https://doi.org/10.36255/exon-publications-breast-cancer-subtypes>
- Ozaslan, M., Karagoz, I. D., Kilic, I. H., & Guldur, M. E. (2011). Ehrlich ascites carcinoma. *African Journal of Biotechnology*, 10(13), 2375–2378.
- Radulski, D. R., Stipp, M. C., Galindo, C. M., & Acco, A. (2023). Features and applications of Ehrlich tumor model in cancer studies: A literature review. *Translational Breast Cancer Research*, 4, 22–22. <https://doi.org/10.21037/tbcr-23-32>
- Rannikko, J. H., & Hollmén, M. (2024). Clinical landscape of macrophage-reprogramming cancer immunotherapies. *British Journal of Cancer*, 131(4), 627–640. <https://doi.org/10.1038/s41416-024-02715-6>
- Royce, M.E.; Osman, D. Everolimus in the Treatment of Metastatic Breast Cancer. *Breast Cancer Basic Clin. Res.* 2015, 9, 73–79.
- Szostakowska, M., Trębińska-Stryjewska, A., Grzybowska, E. A., & Fabisiewicz, A. (2019). Resistance to endocrine therapy in breast cancer: Molecular mechanisms and future goals. *Breast Cancer Research and Treatment*, 173(3), 489–497. <https://doi.org/10.1007/s10549-018-5023-4>
- Taylor, N., et al. (2015). Cactaceae. In *Lista de Espécies da Flora do Brasil*. Jardim Botânico do Rio de Janeiro.
- Telang, N. (2023). Natural products as drug candidates for breast cancer (Review). *Oncology Letters*, 26(2), 349. <https://doi.org/10.3892/ol.2023.13935>
- Zafar, A., Khatoon, S., Khan, M. J., Abu, J., & Naeem, A. (2025). Advancements and limitations in traditional anti-cancer therapies: A comprehensive review of surgery, chemotherapy, radiation therapy, and hormonal therapy. *Discover Oncology*, 16(1), 607. <https://doi.org/10.1007/s12672-025-02198-8>
- Zhang, J., Wu, Y., Li, Y., Li, S., Liu, J., Yang, X., Xia, G., & Wang, G. (2024). Natural products and derivatives for breast cancer treatment: From drug discovery to molecular mechanism. *Phytomedicine*, 129, 155600. <https://doi.org/10.1016/j.phymed.2024.155600>